Modelling of the time evolution of low tropospheric clouds capped by a stable layer

Bent H. Sass

Danish Meteorological Institute

October 1, 2001

Abstract

A numerical study is carried out on the problem of simulating the time evolution of low tropospheric clouds capped by a stable layer. The fundamental processes governing the evolution of boundary layer clouds are briefly reviewed. The numerical investigation is carried out with the physical parameterizations of a weather prediction model (HIRLAM). The role of computing realistic fluxes of moisture and heat near the interface between cloud top and the stable overlying layer is investigated. Two model formulations of these heat- and moisture fluxes are described and tested in 1-dimensional column experiments with specified external forcing. It is shown that the formulation, paying special attention to the exchange process from shallow convection across the interface, can produce realistic entrainment rates of the stable air at the cloud top when tested on observational data from the Atlantic Stratocumulus Transition Experiment (ASTEX). Also the cloud structure and drizzle appear to be better in agreement with observations when compared with the default reference model version. The model formulations are studied further in idealized 1-dimensional tests investigating the effect of different conditions including dynamical forcing specified through vertical velocity varying with height. It is concluded that both the individual physical processes and dynamical forcing play a significant role in the cloud prediction problem. The experiments confirm that subsidence and an upward surface sensible heat flux are strong cloud controlling processes tending to dissipate a cloud once the heating effects have reached a sufficient magnitude. Also the effect of wind shear near cloud top is significant in the revised formulation providing increased heat and moisture fluxes contributing to cloud dissipation. The new formulation does in some situations produce a significantly different simulation of the cloud cover evolution which has implications for weather forecasting .

1. Introduction

The forecasting of boundary layer clouds is recognized to be a difficult task of great importance in numerical weather prediction and climate research (Nicholls, 1984; Albrecht et al., 1995). In particular, the computation of moisture and heat exchange between clouds and an overlying stable layer poses an important and difficult problem in atmospheric modelling and forecasting. This meteorological challenge is well illustrated by the situation where a stratus- or stratocumulus layer is capped by a dry inversion. In numerical weather prediction a correct forecasting of the time evolution of these clouds is important because meteorological forecast parameters such as temperature and precipitation at the ground depend strongly on the cloud evolution. The dependence of the cloud evolution on all major processes such as dynamical forcing, radiation, turbulence, condensation, evaporation and precipitation release (Nicholls, 1984; Duynkerke et al., 1995) is an obvious reason why it is difficult to establish a physically realistic model valid for all atmospheric states. A brief overview of the cloud prediction problem is given in section 2.

The present report is devoted to a 1-dimensional study of how the physical parameterizations of the HIRLAM forecasting system (e.g., Sass et al., 2000) behave when forecasting clouds below a capping stable layer. The simulation time scale covers a range up to 2 days ahead in contrast to a number of studies which are limited to only few hours.

Verification of 3-dimensional cloud fields at the Danish Meteorological Institute (DMI) shows that the frequency of low cloud bases (below 500 m) increases as the forecast length gets longer. This has been revealed from objective verification (a 4 month period) representing data from different seasons. In addition, the verification of precipitation forecasts with the HIRLAM forecasting system at DMI shows that small precipitation amounts are forecasted with a too high frequency (Nielsen and Amstrup, 2001). Moistening below clouds, due to evaporation of small precipitation amounts occurring too frequently, contributes to the risk of cloud formation later on.

One process likely to account significantly for this type of model deficiency is an underestimation of fluxes of heat and moisture at the interface between boundary layer clouds and the stable overlying air. Increased fluxes will tend to moisten the air above the cloud while the specific humidity and cloud water amount in the clouds tend to decrease at the same time. A reduced cloud water amount in the cloud implies less precipitation release and less evaporative moistening in the planetary boundary layer. Based on this reasoning a revised formulation of the moisture and energy fluxes has been developed. The underlying hypotheses and equations are described in section 3.

In section 4 the revised model version is compared with the default reference HIRLAM model physics in 1-dimensional simulations. The first case chosen is based on data from the Atlantic Stratocumulus Transition Experiment 'ASTEX' (Albrecht et al., 1995). The model simulations are supplied with dynamical forcing from subsidence which can be deduced from the ASTEX observational study. The data for this case has previously been used in the HIRLAM collaboration (Holtslag et al., 1999).

Section 4 also includes a study of idealized experiments where the impact of the physical and dynamical processes on the time evolution of cloudy boundary layers is investigated. The realism of the revised formulation of the heat and moisture fluxes between stratocu-

mulus clouds and a capping stable layer is estimated in the light of observational and theoretical studies investigating the processes connected to stratocumulus cloud prediction.

Finally, in section 5 some further discussion on the results is included along with concluding remarks.

2. The cloud prediction problem

We may define a cloud as a part of the atmosphere which is saturated with vapor such as to form hydrometeors, most often water droplets, in a certain concentration. 'Stratocumulus' will be defined to include both broken and unbroken cloud layers below a capping stable layer. The processes governing the evolution of stratocumulus clouds have been studied with increased intensity during the past 3 decades due to the great significance of a cloud topped low troposphere. It has been known for a long time that stratocumulus cloud layers are rather persistent in some climatic regions of the earth. Another characteristic feature is the often sharp 'jump' of atmospheric variables such as specific humidity and temperature between the cloud layer and an overlying dry stable layer. Although it has been clear that several processes are able to affect the evolution of the clouds the details of how physical processes interact and should be described have not been well understood (Nicholls, 1984). The role of the individual physical processes has become increasingly clear in recent years due to comprehensive observational studies, advances in physical meteorology and increased computing power to carry out detailed numerical experiments. However, a precise forecasting of stratocumulus on all time scales from one hour or less to several days ahead is still a big challenge due to the complexity of the problem. Besides the difficulty of describing all important processes in a realistic way the initial state of the atmosphere also needs to be analysed accurately. In addition, numerical issues influencing the accuracy of model computations are a part of the problem to be solved in atmospheric modelling.

The theory of radiative transfer is well developed and has established that strong radiative cooling due to the flux divergence of longwave radiation exists in the upper part of a cloud below a clear sky (Roach and Slingo, 1979; Slingo et al., 1982b). Further down in the cloud the flux divergence due to longwave radiation is small, and near the cloud base heating may occur. Unless the underlying sea- or land surface is warm the total integrated heating of a low tropospheric cloud below a clear sky is strongly negative. Observations and computations of the heating rate in clouds from absorption of solar radiation (Slingo et al., 1982a; Slingo et al., 1982b; Slingo and Schrecker, 1982) show that in midlatitude summer the total vertically integrated heating rate in the middle of the day is barely able to compensate for the cooling due to longwave radiation. The combined effect of longwave radiation and solar radiation is therefore often a net cooling of the cloud. Cooling is however strongly concentrated to the upper part of the cloud. Deeper inside the cloud the combined effect of longwave radiation and solar radiation gives rise to a net heating which contributes to cloud 'thinning' in the lower part and a higher cloud base. Solar radiation is therefore clearly important when forecasting the evolution of cloud base height.

A net cooling effect of radiation in combination with pure condensation of vapor (dis-

regarding other processes such as advection and turbulence) is therefore expected to produce more cloud water since cooling implies supersaturation leading to condensation. In this way radiation in combination with condensation tends to preserve a cloud.

The mutual interaction between radiation and other processes influencing the cloud is however significant. The radiative cooling near cloud top has a strong destabilizing effect with regard to the generation of vertical mixing through turbulence (Duynkerke et al., 1995). On the other hand, the entrainment process of dry warmer air down into the cloud, has a controlling effect on the magnitude of the radiative cooling near cloud top (Randall et al., 1992). The related vertical smoothing of the moisture profile near cloud top tends to reduce the radiative flux divergence and thus the associated cooling rate.

Over the past two decades intensive theoretical discussions and modelling efforts have taken place to quantify the character of temperature and moisture transports across the interface between a cloud and a capping stable layer. In 1980 the theory of 'cloud top entrainment instability' has been published (Randall, 1980; Deardorff, 1980). This hypothesis states that a positive feedback on the turbulent entrainment process at cloud top is established if dry air from the stable layer becomes negatively buoyant in the cloud after it has been cooled to the saturation point by mixing with a volume of cloud air leading to moistening and cooling by evaporation of cloud water. It has been normal practice to associate 'entrainment instability' with cloud dissipation or at least cloud breakup, although it is no proof for it. The following criterion has been derived expressing a condition for cloud top entrainment instability to be realized.

$$\Delta\Theta_e < K_{ctei} \cdot \frac{L}{C_p}\Delta q_t \tag{1}$$

In (1) $\Delta\Theta_e$ and Δq_t are cloud top 'jumps' of equivalent potential temperature and total specific humidity respectively, between cloud and the stable layer above. This means that a sharp change of these variables through a very shallow layer (e.g., 10 m thick) will be described as a discontinuity ('jump') in variables between cloud and the clear atmosphere. A numerically much smaller stable lapse rate can normally be assigned to the atmosphere above the shallow transition layer.

q_t is the sum of specific humditity and specific cloud water. Θ_e and q_t are conserved during an adiabatic condensation and evaporation process. L and C_p are the specific latent heat of fusion and specific heat capacity at constant pressure, respectively. K_{ctei} is a coefficient with a typical value of 0.23, for details see Randall (1980). Numerical experimentation to validate the instability theory for clouds subsequently lead Randall to question the general validity of the proposed criterion (Randall, 1984). He concludes that sometimes the cloud may deepen through increased entrainment under conditions where the cloud should be unstable according to the criterion mentioned above. Also it became clear from observational studies (Albrecht et al., 1985; Kuo and Schubert, 1988) that stable stratocumulus clouds exist in many cases where the criterion (1) tells they should be subject to entrainment instability. Attempts have been made to modify the original theory, and a remarkable contribution has been published in 1990 (MacVean and Mason, 1990). They consider the entrainment as a mixing process between two layers of specified depths which do not have to be equal. The two layers may be saturated

or unsaturated. The case with a saturated lower layer and an unsaturated upper layer is the relevant situation in the present context. The hypothesis states that a necessary condition for entrainment instability is that the net vertically integrated conversion of potential to kinetic energy over the two layers is positive. The concepts to estimate this energy conversion involve linear fluxes of moist conserved variables during condensation and linear buoyancy fluxes in the two layers. It is assumed that phase changes between the two layers occur instantaneously when a volume of air is exchanged between the layers. The same type of relation as (1) has been found, but with a more complex expression for the coefficient K_{ctei}. A typical value of K_{ctei} relevant for stratocumulus cloud is about 0.70 which provides a much more restrictive condition in order to achieve cloud breakup due to entrainment. The revised theory has been shown to be in better agreement with observations. A numerical study has been performed (MacVean, 1993) to investigate if model simulations could produce results consistent with the modified theory. It is noted that in general it is not trivial to define initial conditions for model simulations in order that the simulations produce useful results in the beginning of the model integration. Careful consideration of the experimental conditions is often needed as is apparent from several articles (Bougeault, 1985; MacVean, 1993; Moeng et al., 1995). MacVean concluded (MacVean, 1993), based on his experimentation with a very high resolution 2-dimensional non-hydrostatic incompressible Boussinesq model (typical grid spacing = 4.9 m) , that the experimental results were essentially in agreement with the modified stability criteria.

Several other investigations on the subject of entrainment instability have been more sceptical about the relevance of the criteria for entrainment instability (Siems et al., 1990; Weaver and Pearson, 1990; Wang and Albrecht, 1994)

Observational studies (Slingo et al., 1982b; Albrecht et al., 1985; Rodgers and Telford, 1986; Nicholls and Leighton, 1986; Kuo and Schubert, 1988; Albrecht et al., 1995) using data from satellites, aircrafts and ships, have contributed considerably to enhance the understanding of the processes governing the evolution of stratocumulus clouds despite the problems to eliminate uncertainties on the subject of cloud top entrainment instability.

Several studies have confirmed that turbulent exchange of heat and moisture between the cloud and a stable layer is often very significant as measured by the entrainment velocity W_e. This is the velocity describing how fast the cloud top would move vertically (in the absence of a larger scale subsidence velocity) due to entrainment mixing of the clear air at cloud top down into the cloud. Nicholls and Leighton (1986) presented the results of six flights with instrumented aircraft investigating the properties of marine stratocumulus clouds around the British Isles. The entrainment velocities for the six cases lie in the range from 0.24 cm s^{-1} to 0.71 cm s^{-1}. The entrainment estimated during the ASTEX experiment generally lies in the range from 0.4 cm s^{-1} to more than 1.0 cm s^{-1} (Bretherton et al., 1995; Duynkerke et al., 1995). It may be concluded that values deduced from observations indicate entrainment rates of several hundred metres per day for stratocumulus clouds.

Another rather common feature of stratocumulus is that the mixing process in connection with the clouds may be disconnected from the turbulence processes close to the

land- or sea surface (Nicholls and Leighton, 1986; Turton and Nicholls, 1987). In other words, it is decoupled from the surface layer turbulence. In the study of Nicholls and Leighton (1986) decoupling occurred at some level below cloud base in four out of six cases. Also during ASTEX decoupling appeared to occur often (Albrecht et al., 1995). The two turbulent layers may however reconnect. This happens when cumulus clouds rise into stratocumulus (Wang and Lenschow, 1995). Some cumulus clouds are able to penetrate the stratocumulus cloud top. Wang and Lenschow studied this effect of cumulus penetrating a stratocumulus layer during ASTEX. They concluded that there are indications that the entrainment rate of the stratocumulus layer is increased in the presence of penetrating cumulus. The cumulus clouds act as an additional source of moisture for the stratocumulus layer which is also mentioned in the study of Bougeault (1985). The decoupling process has been studied by Turton and Nicholls (1987) who find that decoupling is favoured by absorption of solar radiation in the lower part of the cloud layer and by a small surface buoyancy flux. They emphasize that the diurnal variation of the depth of stratocumulus becomes larger in the case of decoupling. This is because of the lack of moisture supply from below. As a consequence solar heating effects can better lead to reduced cloud water amounts and a higher cloud base. Also Bougeault (1985) showed in his numerical simulation of marine stratocumulus with a higher order turbulence scheme that decoupling could be reproduced as a transient phenomenon in the context of the diurnal cycle.

As mentioned above, the theory of cloud top entrainment instability has attracted a lot of attention. However, some of the observational studies have made it clear that stratocumulus may dissipate in many situations where entrainment instability could not have been the responsible process. A number of studies have emphasized the importance of other processes.

Kuo and Schubert (1985) in their numerical study of cloud breakup speculate that other processes may counteract cloud top entrainment destabilization. For example, surface evaporation, which was not included in their numerical simulation, is a source of moistening affecting the moisture budget of the cloud. Weaver and Pearson (1990) stress the importance of other processes than cloud top entrainment in the cloud evolution process. In particular they emphasize the effect of subsidence as a very important mechanism for cloud breakup. They present cases with strong indications of subsidence as the responsible mechanism for the process for break up of boundary layer stratocumulus. An observational study of stratocumulus evolution over land (Price, 1999) demonstrates that both an upward sensible heat flux due to the diurnal heating cycle and wind shear through cloud and the stable layer above can be important for stratocumulus breakup. The importance of shear driven turbulence even in the case of strong radiative cooling at cloud top has also been demonstrated by others (Duynkerke and Driedonks, 1988).

It is therefore consistent with several investigations to claim that a realistic forecasting procedure for the evolution of stratocumulus requires that all significant processes contributing to the moisture and energy budget of the cloud layer are treated carefully.

3. Model formulation of the moisture and heat exchange between cloud and the stable layer

The experiments carried out in the present study are made with a column version of the HIRLAM physical parameterizations (e.g., Sass et al., 2000).

Dynamical forcing can be specified and computed in the following way: The 1-D dynamics operate through the computation of a coriolis-acceleration and a specified pressure gradient. Also horizontal advective tendencies may be imposed. A vertical velocity profile may be specified, which is important in the present study, since it is relevant to investigate the effect of subsidence on stratocumulus development. The effect of vertical advection is computed from the vertical gradient of the model variable using an upstream advection. In addition, the heating effect from vertical motion due to compression is included.

The physical parameterizations include all the important processes to study stratocumulus, that is, the parameterization of

- surface fluxes of latent heat, sensible heat and momentum (interactively computed or specified)
- solar radiation and longwave radiation using a highly parameterized scheme.
- condensation, precipitation and evaporation of precipitation or cloud water.
- turbulent and convective transports of heat, specific humidity, cloud water and momentum.

The vertical transports of heat, specific humidity and cloud condensate are key processes in the present study. The turbulence scheme describes the subgrid scale fluxes of heat, moisture and momentum in the framework of 'turbulent kinetic energy' as a prognostic variable in addition to other conventional model variables. This scheme originates from a general formulation (Cuxart et al., 2000) which may be used for mesoscale models, as well as for large-eddy models. The scheme is originally formulated in the framework of moist conserved variables, but the present implementation in the HIRLAM physics (see for example Sass et al., 2000) utilizes instead temperature, specific humidity and cloud condensate as three prognostic variables.

The turbulence- and condensation processes are currently made in three steps. First are the vertical transports of potential temperature, specific humidity and cloud condensate computed by the turbulence scheme. Adjustments to the vertical transports of these variables are then performed in a second step by the convection scheme which takes into account latent heating effects from vertical subgrid scale transports. Finally, the stratiform condensation describes the additional condensation arising as a consequence of the vertical subgrid scale transports. This third part of the processing computes a supersaturation determined from a saturation specific humidity. Symmetric functions of moisture variables around the grid box mean value determine the rate of condensation.

The default convection scheme (January 2001) has a convective closure based on moisture convergence (Sass et al., 2000) and the simple cloud ascent model does not allow for convective moisture and heat transport above the level of transition to negative buoyancy at the top of convective clouds. This has consequences for the treatment of

stratocumulus clouds because the only transports across the stable layer at cloud top can arise from the turbulence. Too small turbulent transports are indeed to be expected when using the current version of the turbulence scheme, because it is formulated in terms of 'dry variables' and not by variables conserved during condensation processes. As a consequence, the mixing length formulation, based on buoyancy arguments in a non-saturated environment, is probably too small in most situations when applied to cloudy conditions.

Therefore, a simple but physically sound extension to the formulation of the subgrid scale heat- and moisture transports is described. This extension stays within the framework of the current philosophy of separating vertical subgrid transports and condensation computations in the three steps mentioned above.

We let the convection scheme describe the effect of larger turbulent eddies in an environment where condensation takes place. The computations make use of the cloud parcel ascent computation of the convection scheme. Physically we may think of the heat- and moisture transports as accomplished by mainly the larger eddies penetrating through the stable layer on top of a cloud layer. The penetration of these eddies into the stable layer can be estimated from the cloud parcel ascent. The observational evidence that stratocumulus are associated with a substantial entrainment of (dry) air from the stable layer into the cloud makes it reasonable to assume that this hypothesis of 'overshooting' eddies as the mechanism for entrainment of dry air is a reasonable concept. We denote by w_b a characteristic vertical velocity of convective motions in the cloud right below the cloud top and will estimate a distance D of penetration into the stable layer. The maximum fluctuation s' of the variable s possible at the interface between cloud and the stable layer is estimated to be approximately equal to the increase above the value s_- at the interface on the cloudy side up to the value s_D at depth D into the stable layer. The value s_D is estimated from the mean gradient of the variable at cloud top. More specificly, it is assumed that the flux at the cloud top of the scalar s is a factor $\tilde{w}$ times s'. It is reasonable to assume that the velocity scale $\tilde{w}$ is closely linked to the subgrid scale kinetic energy E already computed in the model. It is therefore argued that a reasonable estimate is

$$\tilde{w} = K_* \cdot \sqrt{E} \tag{2}$$

In (2) $K_* = 0.25$ has been determined on the basis of numerical experimentation.

The depth of penetration D into the stable layer is estimated as follows: From dimensional analysis it has been argued that the vertical velocity w_r of an idealized thermal depends on its size r, the dimensionless buoyancy B of the 'bubble' and the acceleration of gravity g (m s^{-2}) according the following combination (Rogers, 1976).

$$w_r = c\sqrt{gBr} \tag{3}$$

In (3) B is the virtual temperature difference between the cloud parcel and environment, divided by the environmental temperature. c =1.2. Choosing r = 50 m as representing the dimension of convective eddies near cloud top we get

$$w_b = w_0 \cdot \sqrt{B}$$

$w_0 = \approx 27$ m s^{-1}.

B is computed in the cloud ascent of the convection scheme. It is noted that the turbulent kinetic energy E appearing in (2) is assumed to be no less than $1.0B\mathrm{m}^2$ s^{-2} in order to avoid a risk of very low values with the present turbulence scheme in the case of a small wind shear.

We estimate the maximum penetration depth D from the deceleration in the stable layer. Utilizing the start velocity of w_b for the deceleration we get

$$D = w_0 \sqrt{\frac{B \cdot T}{g|\gamma_c - \gamma|}} \tag{4}$$

In (4) D is in metres, T is temperature (K), γ_c in K m^{-1} is the lapse rate associated with moist adiabatic ascent ($\gamma_c > 0$) and γ in K m^{-1} is the ambient lapse rate in the stable layer. It is demanded that $\gamma < \gamma_c$. A numerical security computation has been implemented to avoid extreme behaviour if the two lapse rates become almost equal, and the penetration is not allowed to exceed a depth corresponding to 25 hPa. The sensible heat flux F_H (J m^{-2} s^{-1}) at the level of transition between cloud and the stable layer is computed according to

$$F_H = \rho C_p \cdot \tilde{w} \cdot D \cdot \frac{\partial \theta}{\partial z} \tag{5}$$

In (5) C_p is the specific heat capacity at constant pressure. ρ is air density, θ is potential temperature.

Similarly we get for the moisture flux of total specific humidity q_t (kg$_{\mathrm{water}}$ m^{-2} s^{-1}) at the transition level

$$F_{q_t} = \rho \cdot \tilde{w} \cdot D \frac{\partial q_t}{\partial z} \tag{6}$$

We assume that the fluxes of heat and moisture determined from the above formulas are distributed linearly with height in the convective cloud of depth D_- and in a stable layer D_+. The latter should approximately be equal to D apart from the constraints set by vertical resolution. If D is larger than the depth of one model layer above cloud a sufficient number of levels are included to exceed D. Currently specific humidity q and cloud condensate q_l are processed independently according to the method described above, but the flux of the moist conserved variable of 'total specific humidity' is then also linear, which preserves moisture structures in a well mixed cloud.

A semi-implicit treatment of the scheme has been introduced to reduce the risk of noise or instability when computing updates of the prognostic variables. It involves partial derivatives of the fluxes described above, as well as the associated layer depths.

4. 1-dimensional tests with specified forcing

This section describes the results of 1-dimensional column tests with the model versions of the HIRLAM physics mentioned above. The task of giving an 'in-depth' treatment of all important processes involved in stratocumulus-forecasting is obviously enormous. Here the choice has been made to investigate three cases in some detail.

We start by simulations related to ASTEX (case 1 below) and continue with a number of idealized tests investigating the effect of different processes on the evolution of stratocumulus. One set of experiments (case 2) represents unstable conditions with respect to the MacVean & Mason criterion.

Another set of experiments (case 3) represents stable conditions. For each case, defined by the initial conditions, the cloud evolution is studied for different dynamical forcing conditions involving a constant or a time varying geostrophic wind. Also the influence of subsidence and specified surface fluxes of sensible and latent heat is investigated. All simulations have been run with a time step of 5 min. The model subgrid scale condensation (Sass et al., 2000) starts at a threshold relative humidity depending on the height above the surface and on the horizontal model resolution. Hence a formal choice (0.15 °) is made for the horizontal resolution even in the context of the 1-D experiments. The threshold relative humidity for the stratocumulus experiments is typically around 95 %.

4.1. The ASTEX case

The ASTEX experiment (Atlantic Stratocumulus Transition EXperiment) was a comprehensive international regional project connected to the International Satellite Cloud Climatology Project ISCCP (Albrecht et al., 1995). This involved coordinated measurements from aircraft, satellites, ships, and islands in the area of the Azores and Madeira Islands in the North Atlantic. The goal has been to provide data sets which could serve as a basis for research on various aspects of the physics of stratocumulus. The experiment was conducted from 1-28 June 1992. The data set tested has been constructed for 1-dimensional tests. It is valid for a 15 hour period on 13 June 1992. This period was characterized by a relatively well mixed boundary layer and no decoupling. A rather large entrainment rate, approximately in the range from 0.6 -1.0 cm s^{-1} has been diagnosed from different methods, as mentioned later. A linear increase of subsidence with height above the surface is specified, reaching a constant value of 0.75 cm s^{-1} at a height of 1500 m. This corresponds approximately to a constant divergence of $5 \cdot 10^{-6}$ s^{-1} in that part of the atmosphere. The surface pressure is taken to be 1029 hPa. The geographical latitude is 37° N. The geostrophic wind components U_g, V_g =(-2,-10) m s^{-1} are constant in the vertical and in time for the experiment. The surface fluxes are specified and fixed during an experiment. The latent heat flux is 30.6 W m^{-2} directed upwards, and the sensible heat flux is small upwards and equal to 12.4 W m^{-2}. The surface friction velocity equals 0.09 m s^{-1}. The initial profiles of temperature, wind components, specific humidity and cloud water using 40 levels, have previously been constructed for HIRLAM purposes (Holtslag et al., 1999). A number of 8 model levels are used below 1000 m. Another 8 levels are used approximately for the next kilometre of the atmosphere. The initial profiles of liquid water (q_l) and 'liquid water potential temperature' (Θ_l) are shown in fig.1.

$$\Theta_l \approx \theta - \frac{L}{C_p} \cdot q_l \tag{7}$$

In (7) θ is the potential temperature. The relative humidity and the model deduced cloud cover profiles are shown in fig.2.

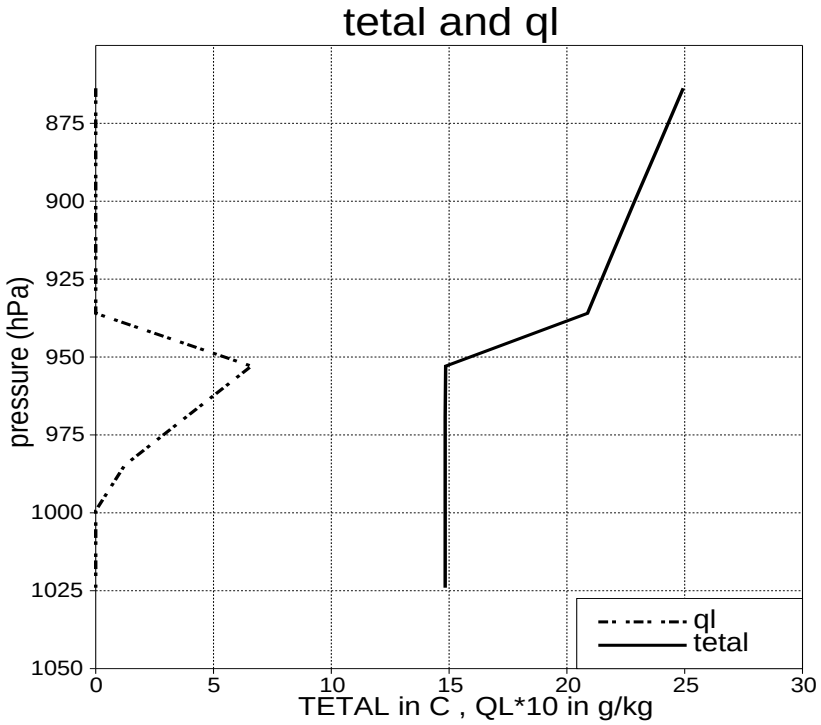

Figure 1: Initial profiles of specific cloud water and liquid water potential temperature for the ASTEX simulation.

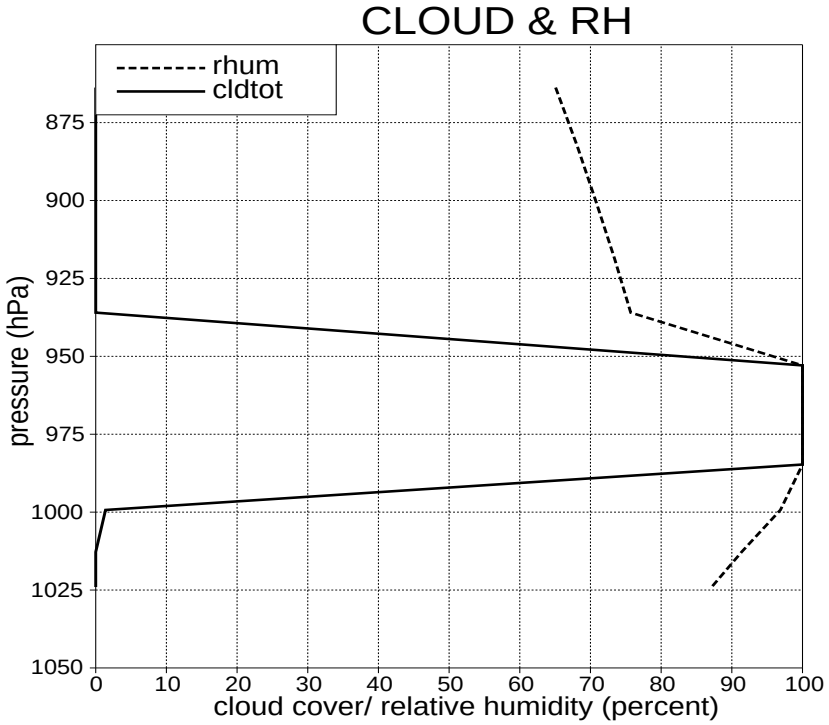

Figure 2: Initial profile of relative humidity and fractional cloud cover for the ASTEX experiment.

It is seen that the cloud is about 60 hPa deep with a cloud base starting close to 1000 hPa. The specific cloud water amounts to about 0.00065 kg_{water} kg^{-1} near the cloud top. The liquid water potential temperature is almost 15 °C in the (well mixed) layer from the surface to the cloud top where the temperature rises by about 3 °C to the next model level.

In fig.3 the profiles of cloud liquid water and of liquid water potential temperature are shown after the simulation time of 15 hours. REF stands for the reference experiment, and NEW stands for the revised model including the effect of shallow convection. The corresponding vertical profiles of fractional cloud cover are shown in fig.4.

From the vertical profiles of cloud water in fig.3 it is seen that the reference run produces a stable cloud position with a slight increase of the cloud water amount at the top when compared to the original amount (fig.1). On the other hand NEW is associated with a cloud top lifting and some decrease of the specific cloud water at the top, approximately to a value of 0.5 g_{water} kg^{-1}.

If we assume, as a first approximation, that the evolution of the position of cloud top height closely reflects the entrainment velocity W_e, we may estimate the latter from the results of fig.3 and fig.4, provided that subsidence is taken into account. Since we impose a subsidence velocity linearly increasing to 0.75 cm s^{-1} at 1500 m, it is possible to estimate that the cloud top sinking due to vertical advection should be approximately 220 m in 15 hours. A simple interpretation of the reference experiment therefore is to assume an entrainment rate of roughly equal magnitude to make the cloud stationary, that is, $\approx$ 0.4 cm s^{-1}= 350 m day^{-1}.

For the modified model formulation (fig.4) it is less obvious how to make the estimate because of fractional cloudiness near the top. One procedure is to follow the evolution of the position of the level with approximately 100 percent cloud cover, which has moved with a velocity of $\approx$ 0.70cm s^{-1}. Also the changed position of the first vertical level where cloud cover has decreased to zero may be taken into account. If a 50 percent weight is chosen to both of these changed positions, the entrainment rate becomes about 0.86cm s^{-1}.

A proper assessment of the entrainment velocity normally requires that fluxes at the cloud top from turbulence plus convection are computed. A frequently applied method is to compute W_e according to the flux of total specific humidity (specific humidity plus specific cloud water) at cloud top, divided by the vertical change (jump) of the same quantity between cloud top and the air above, see for example Bougeault (1985):

$$W_e = \left(\frac{\overline{w'q'} + \overline{w'q_l'}}{\Delta q_t}\right) \tag{8}$$

In (8) q and q_l are specific humidity and specific cloud water respectively. $q_t = q + q_l$. Computations based on (8) for both experiments mentioned above gives W_e =0.57 cm s^{-1} for the reference simulation and W_e =1.00 cm s^{-1} for the revised scheme. These values represent a fair agreement with the first estimates. A direct computation of entrainment is not completely trivial because the cloud top is non-stationary, and the computation is sensitive to how Δq_t at cloud top is computed. The method suggested by Bougeault (1985) to compute the difference over two grid lengths has been used.

Although the computation is rather noisy on an individual time step basis it is feasible when integrated over one or several hours , in this case 15 hours.

The model computed entrainment rates obtained with the new scheme agree well with the entrainment velocity obtained in the diagnostics based on measurements (Bretherton et al., 1995).

Three different methods to estimate the entrainment velocity have been mentioned in the study of Bretherton et. al (1995). The first method is based on ECMWF synoptic-scale analyses of vertical motion, coupled with the observed rate of change of inversion height, following the mixed boundary layer air column. The method gave a mean estimate of 0.9 cm s^{-1} for the entrainment velocity W_e. The second method is based on calculating the entrainment drying as a residual in the water budget of the mixed boundary layer air column. The third estimate has been deduced from ozone fluxes measured just below the entrainment interface and ozone jumps across the inversion. The mean estimate of W_e from the second and the third methods are 1.0 cm s^{-1} and 0.6 cm s^{-1}, respectively. The estimated uncertainty for the different methods is up to 0.5 cm s^{-1}. The authors point out that a value for W_e=0.7 cm s^{-1} is consistent with estimates from all three methods. Based on these diagnostics it appears that the reference 1-D experiment (REF) is associated with too little entrainment of inversion air while the results of the revised formulation (NEW) are in good agreement with the estimate from measurements.

It is also natural to investigate the evolution of liquid water potential temperature. This quantity is conserved in a moist adiabatic process and is normally almost constant for a solid stratocumulus cloud layer. The results of the reference experiment show that this temperature is lowered, by less than 1 °C near the sea surface to almost 2.5 °C near the cloud top. This cooling at a level around 950 hPa does not appear to be realistic as compared to the data from ASTEX (Bretherton and Pincus, 1995). The measurements indicate that the temperature change should be less than about 1 °C which is in agreement with the NEW experiment. Higher up, at about 920 hPa a substantial cooling is observed which has also been reproduced in the modified scheme. A large cooling of about 5 °C at levels which were initially well above cloud top and later near the top has also been reproduced in other numerical studies of entraining stratocumulus, see for example fig.3 of Bougeault (1985). Furthermore, the measured values of cloud water amount near cloud top appear to be somewhat decreasing during June 13th 1992 which supports the slow decrease forecasted in NEW.

The evolution of accumulated precipitation in the two experiments is shown in fig.5. It is seen that both experiments are associated with precipitation. The modified scheme simulates less precipitation, that is, an average precipitation rate close to 1 mm day^{-1}.

The measured values show a significant variability in time but the time averaged intensity appears to be around 1.0 mm day^{-1} (Bretherton et al., 1995). The reference experiment computes an average intensity of about 1.8 mm day^{-1}, which appears to be higher than observed.

We also display the time averaged temperature changes due to the different processes in the two experiments. Fig.6 displays the results for REF while the results for NEW are shown in fig.7. We see that the parameterization of additional heat- and moisture

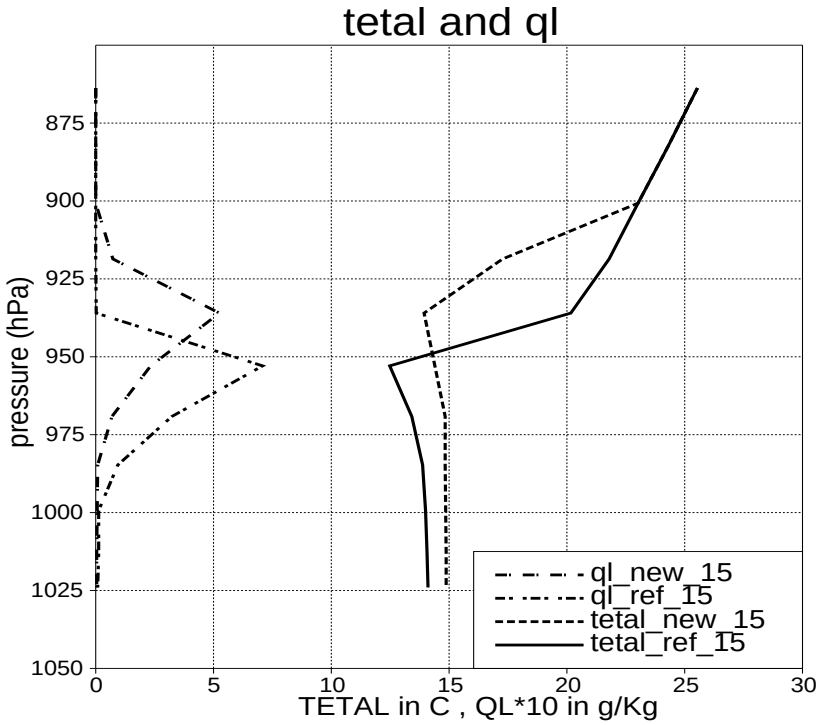

Figure 3: Vertical profiles of liquid water potential temperature and specific cloud water in ASTEX simulation after 15 hours using model versions REF and NEW.

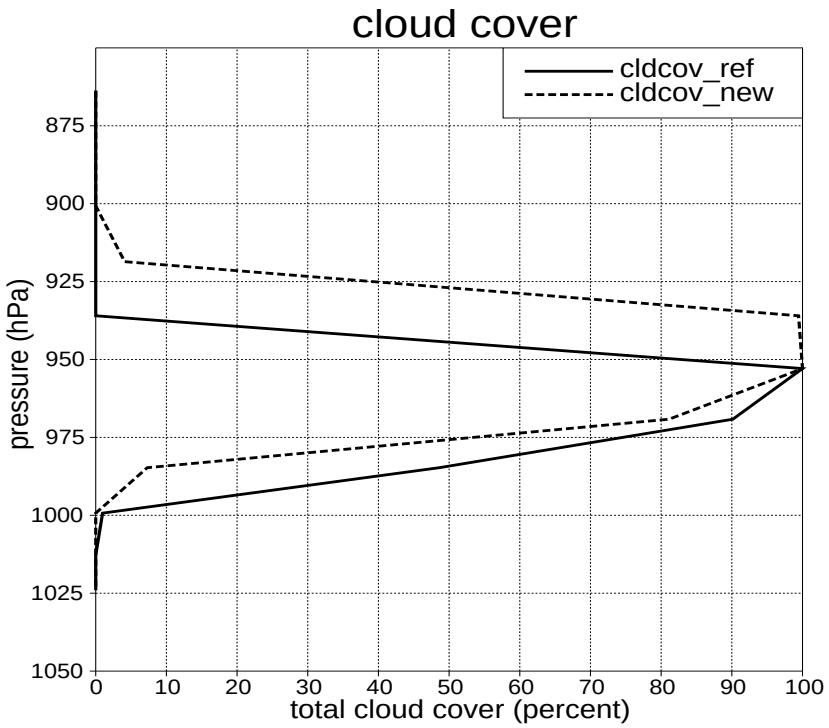

Figure 4: Vertical profiles of total cloud cover in ASTEX 15 hour simulation. 'ref' applies to reference simulation and 'new' to the new scheme.

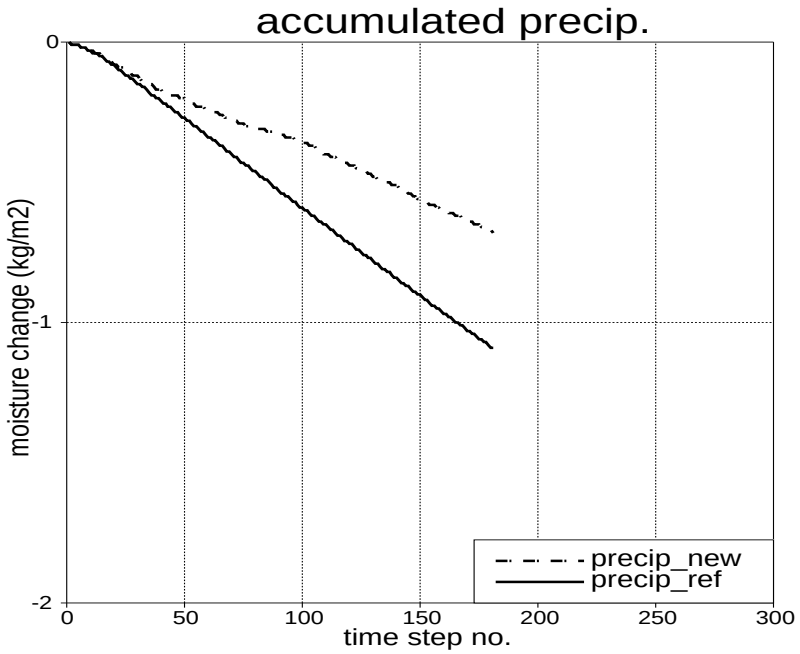

Figure 5: Accumulated precipitation as a function of time for the default scheme (solid line) and for the new version of the convection scheme (dashed line)

transports across the interface between cloud and the dry inversion leads to a substantially modified participation of heating/cooling as a result of the individual processes. The 'shallow' convection is counted as convection which is included in 'dtcond' in the figure. This curve ('dtcond') also includes the heating effect of all condensation related processes, including also stratiform type of condensation. In both experiments, the main governing processes are the oppositely acting processes of longwave radiative cooling and heating due to condensation and convection. The peak amplitudes of these key processes are reduced in NEW due to a vertical averaging, as a consequence of the fact that the cloud top is moving upwards to a higher level during the forecast period. Note that in REF a balance above cloud is approximately established between cooling due to radiation and heating due to subsidence. In NEW, however, the most important processes above cloud appear to be heating due to subsidence and cooling due to evaporation of cloud water flux from shallow convection and from sensible heat divergence (a downward heat flux gives rise to cooling). Below the cloud we may interprete results such that cooling due to evaporation of precipitation is relatively more important in REF as compared to NEW. This is also in agreement with larger precipitation in REF and with the original hypothesis stated in the introduction, that evaporative cooling below cloud is of importance in the reference model version. The heating from turbulence close to the surface to compensate for radiative cooling is prominent in both simulations.

4.2. Other experiments (Case 2)

The role of different processes and of model resolution are investigated in the experiments described below. For Case 2 all experiments are based on initial conditions describing a vertical variation of humidity and temperature around cloud top associated with a stability coefficient $K_{ctei} = 0.80$. According to the Mason & McVean criterion

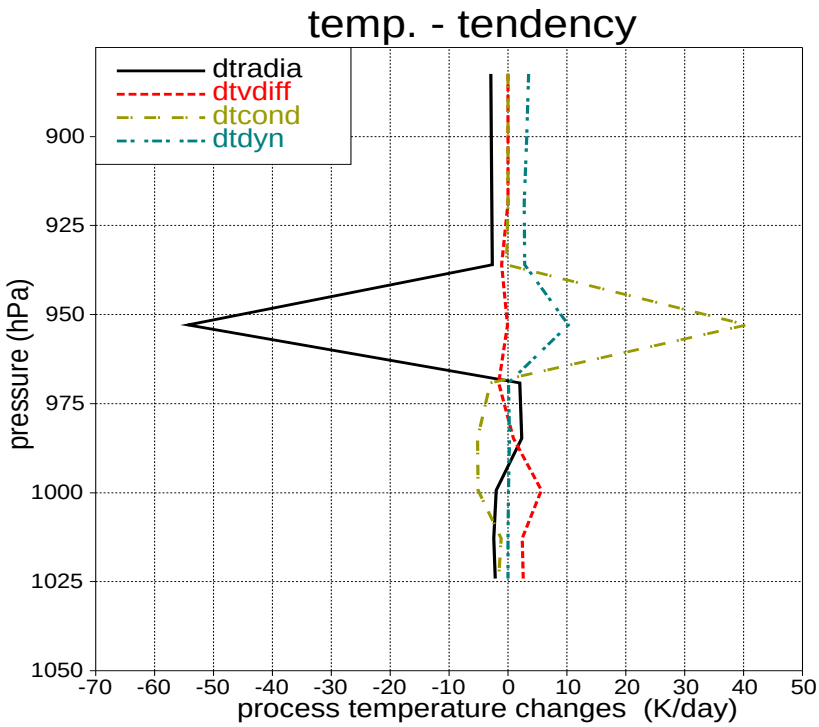

Figure 6: Temperature tendencies time averaged over 15 hours of the ASTEX simulation showing profiles due to radiation (dtradia), condensation (dtcond), turbulence (dtvdiff) and dynamic forcing (dtdyn) valid for the default model version

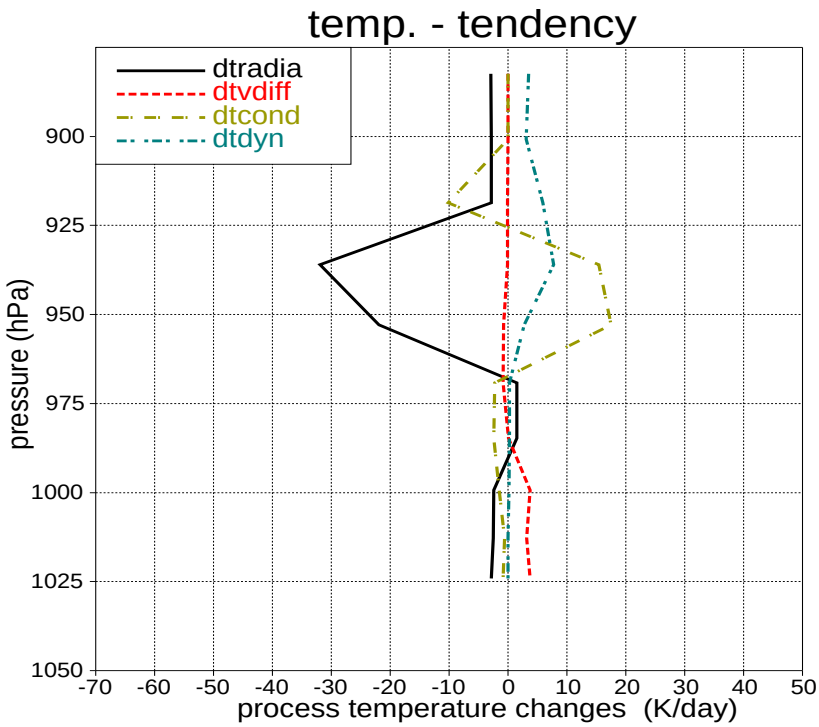

Figure 7: As in fig.6, but for the new version of the convection scheme to enhance fluxes across the capping stable layer.

this value should provide the conditions for mixing instability when chosen to define the ratio between $\Delta\Theta_e$ and Δq_t.

The initial conditions are specified below cloud top by linear functions used for temperature, relative humidity and cloud water as a function of height. Experiments are carried out using 40 vertical levels. Once a specific vertical resolution is chosen, the initial conditions of temperature, relative humidity and cloud water are determined from the analytical description defined by the linear functions. The initial profiles of liquid water (dashed) and liquid water potential temperature (solid curve) are shown in fig.8. The vertical resolution is determined from the following power function defining the hybrid sigma levels b_k

$$b_k = \left(\frac{k-1}{N}\right)^c \tag{9}$$

In (9) k is the vertical level number (half level), N in the number of model levels (full levels) and c is a real number chosen for the power function. Three resolutions (LOW, MED and HIG) are tested using $c = 0.66$, 0.33 and 0.11, respectively. The surface pressure is chosen to be 1013.25 hPa. These resolutions correspond to approximately 7, 12 and 25 vertical levels in the lowest kilometre of the atmosphere.

The situation is considered with of a cloud initially between 500 m and 1000 m above the surface, which is assumed to be a sea surface. The initial temperature of the lowest model layer is chosen to be 290 K, and the relative humidity is 80 percent. The temperature decrease with height in the lowest kilometre is initially assumed to be 0.007 K m^{-1}. The relative humidity becomes 100 percent between 500 m and 1000 m. The specific cloud water amount is assumed to increase linearly from bottom to top in the cloud, reaching a maximum close to $0.5 g_{water}$ kg^{-1} at the cloud top.

For all resolutions the associated jumps of temperature, specific humidity and cloud water to the first level above cloud top are determined such as to produce $K_{ctei} = 0.80$. Levels higher up are assumed to have constant values of temperature, specific humidity and cloud water. The latter has a value of zero corresponding to cloud free conditions.

A strategy for specifying the initial wind profile and the forcing through the geostrophic wind and possibly horizontal and/or vertical advections needs to be established. Since the primary purpose of the present study is to investigate the vertical transports, it is desired to obtain a situation where horizontal advections of the dependent variables are approximately zero. This can be obtained if the geostrophic wind is assumed quasi-constant with height at any time. A small vertical variation is computed according to the thermal wind relation to make the horizontal temperature gradients vanish (zero horizontal temperature advection). The effect of a constant and small geostrophic wind is examined, and the effect of gradually increasing the pressure gradient linearly in time. All experiments are started with initial winds equal to a small geostrophic wind (5m s^{-1}). This enables that there will be only little spinup of the wind profile (over sea). Experiments with increasing pressure gradient as a function of time will then simulate a transient situation in the atmosphere with developing wind shear. The heating and advection associated with a linear variation of vertical velocity with height is examined in a separate experiment. The experiments described in some detail below have been made for a situation with no solar heating (geographical latitude chosen to be 75°N). The impact of various surface fluxes of sensible and latent heat is investigated. These

fluxes are specified as time independent. The momentum flux is allowed to evolve as a consequence of the wind forcing, using drag formulas and a variable roughness length in agreement with Charnock's formula (Charnock, 1955).

4.2.1. Forcing from a weak constant pressure gradient

In this experiment (2.1) the surface geostrophic wind is fixed in time and is only 5 m s^{-1}. There is no vertical subsidence velocity imposed and the surface fluxes of sensible and latent heat are forced to be zero.

The results of the simulations using the different resolutions mentioned above are presented in table 1a and table 1b. The first table shows the 24 hour accumulated precipitations for the two model versions and the different vertical resolutions. Table 1b displays the actual changes (hPa) in cloud top heights realized during the simulations covering a forecast range from 12 hours to 48 hours. The first number in table 1b applies to a result obtained with the new scheme while the numbers in parentheses correspond to a result of the default simulation. In the subsequent discussion these numbers will be interpreted as representing entrainment rate, due to a reasonable agreement with a direct computation, as mentioned for the ASTEX case. Also shown is the development over 24 hours (experiment HIG) of the vertical profiles of liquid water potential temperature and liquid water. Fig.8 applies to the reference experiment while fig.9 corresponds to the results of the new scheme.

It is first noted that in both experiments the cloud and sub-cloud layers are cooled (up to about 2°C. This is not surprising since a strong radiative cooling is present at cloud top while the surface energy fluxes have been set to zero. Since there is no heating from subsidence the radiative flux divergence in the vertical gives rise to cooling. We also note that the cloud does not break up or dissolve (consistent with figures 8 and 9). A discussion on this issue is postponed until section 5. At this stage we note some characteristic differences between fig.8 and fig.9 of the high resolution runs. It is clear that more entrainment is associated with experiment NEW, as compared to REF. This has several important consequences. In REF the cloud top liquid water amount increases during the 24 hours and the cloud is not 'well mixed' as far as the profile of Θ_l is concerned. In NEW, however, the liquid water decreases somewhat during the integration and Θ_l increases slightly near cloud base while a modest decrease is seen near the cloud top. The substantial decrease of Θ_l towards cloud top in REF is not considered to be realistic and is in conflict with quasi-constant profiles generally seen in observational studies , see for example Nicholls (1984) and Nicholls and Leighton (1986). The lack of a proper entrainment at cloud top is an important reason for this result. The entrainment, as simulated by the new shallow convection scheme, supplies heat to the cloud layer. This process counteracts cooling of the top part of the cloud and tends to reduce the liquid water near the top. Near the cloud base the heat flux from above gives rise to a modest increase of Θ_l. This means that a cloud 'decoupling' has been simulated, that is, a stable layer near cloud base is established. As mentioned in section 2, small surface buoyancy fluxes (in this case zero surface sensible heat flux) are believed to favour cloud decoupling. As most experiments mentioned below are carried out for

zero surface fluxes of sensible and latent heat there will be more results showing decoupling in the subsequent experiments. The accumulated precipitations of table 1a show a modest reduction of precipitation with NEW as compared to REF (0.77 mm versus 1.08 mm at a high resolution). This is consistent with the reduced liquid water amount at cloud top in NEW since precipitation release is essentially dependent on a specific cloud water threshold to be exceeded in order that precipitation release can become efficient. The sensitivity of accumulated precipitation to resolution is modest. A few comments should be given to the results of table 1b. We see that continued entrainment occurs beyond 24 hours. It is seen that for NEW the entrainment is not very different in medium and high resolution (70 hPa in 48 hours). However, a weak entrainment is produced in low resolution (15 hPa in 48 hours). This type of problem seems to be linked together with small surface fluxes and small vertical wind shear as discussed later.

Table 1a :
Accumulated 24 hour precipitation for experiment 2.1 run with forcing from a weak and constant pressure gradient. REF applies to unmodified scheme, NEW to the modified scheme. LOW, MED and HIG apply to a coarse, medium and a high vertical resolution respectively (see text)

model/res.	LOW	MED	HIG
REF	1.02	1.07	1.08
NEW	0.93	0.86	0.77

Table 1b:
Accumulated cloud top lift (hPa) for experiment 2.1 (see text). Numbers in brackets apply to the unmodified scheme. Results are shown for forecast lengths of 12, 24, 36 and 48 hours. LOW, MED and HIG apply to a coarse, medium and a high model resolution (res), respectively.

fclen/res.	LOW	MED	HIG
+12 h	+15 (0)	+20 (10)	+15 (15)
+24 h	+15 (15)	+45 (20)	+45 (15)
+36 h	+0 (15)	+55 (20)	+70 (25)
+48 h	+15 (15)	+70 (20)	+70 (25)

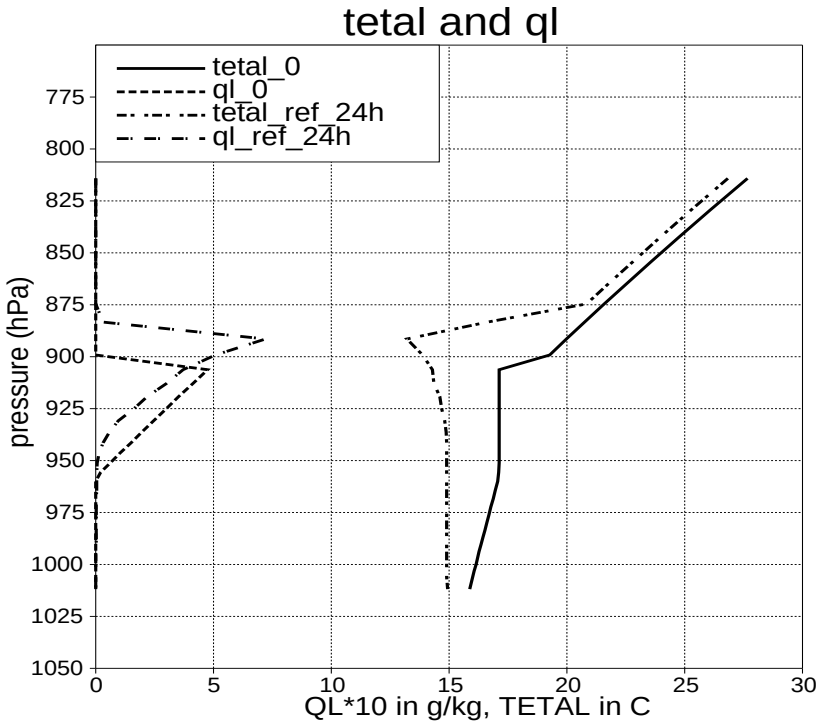

Figure 8: Vertical profiles of cloud condensate and liquid water potential temperature at initial time and at 24 hours forecast length for experiment 2.1 (REF) using the high vertical resolution HIG (see text)

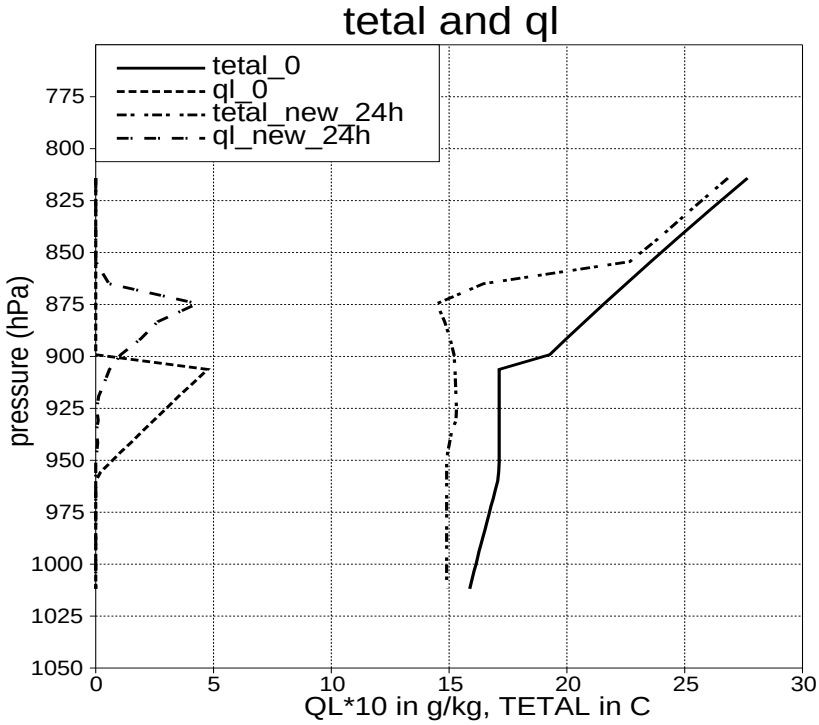

Figure 9: Vertical profiles of cloud condensate and liquid water potential temperature at initial time and at 24 hours forecast length for experiment 2.1 (NEW) using the high vertical resolution HIG (see text).

4.2.2. Forcing from a moderately increasing pressure gradient

The experimental conditions of this experiment (2.2) are similar to that of the previous one (2.1) except that the surface geostropic wind is increased linearly in time with 10 m s^{-1} over 24 hours, becoming 15 m s^{-1} at +24 hours. It represents a nonstationary situation with the development of some wind shear (not shown). The results are presented in tables 2a , 2b and in figures 10 and 11 showing corresponding results to those presented in experiment 2.1.

Most of the results are qualitatively similar to those of 2.1 : More entrainment and a more well mixed cloud layer with NEW compared with REF. It is noted that a small 'dip' (decrease) in Θ_l is still present in NEW (top layer). This feature is also seen in several other simulations of stratocumulus with models including physics using 3rd order turbulence closure schemes (Chen and Cotton, 1983; Bougeault, 1985). One may state that it is a challenge for the model describing the vertical transports of heat and moisture, above and below cloud top, to compensate for the large infrared cooling rate in the uppermost part of the cloud. A verification of this feature in observational studies is difficult due to the horizontal variability of cloud top heights as seen by the aircrafts providing the measurements. The precipitation amounts (table 2a) for this experiment are very similar to those for experiment 2.1. However, the entrainment rates are generally increased. This effect comes from wind shear giving rise to increased downward heat transport. This effect can be identified on the profiles of Θ_l which are somewhat warmer than the corresponding ones for experiments 2.1 . Moreover, the large difference between the entrainment rate for LOW as compared to MED and HIG using the new scheme is significantly reduced.

Table 2a :
Accumulated 24 hour precipitation for experiment 2.2 run with forcing from a moderately increasing surface pressure gradient. REF applies to unmodified scheme, NEW to the modified scheme. LOW, MED and HIG apply to a coarse, medium and a high vertical resolution respectively (see text)

model/res.	LOW	MED	HIG
REF	1.07	1.19	1.20
NEW	0.98	0.79	0.77

Table 2b:
Accumulated cloud top lift (hPa) for experiment 2.2. Numbers in brackets apply to the unmodified scheme. Results are shown for forecast lengths of 12, 24, 36 and 48 hours. LOW, MED and HIG apply to a coarse, medium and a high model resolution (res) respectively.

fclen/res.	LOW	MED	HIG
+12 h	+15 (15)	+20 (10)	+15 (15)
+24 h	+35 (15)	+45 (20)	+45 (15)
+36 h	+50 (15)	+70 (20)	+85 (35)
+48 h	+70 (35)	+95 (45)	+105 (45)

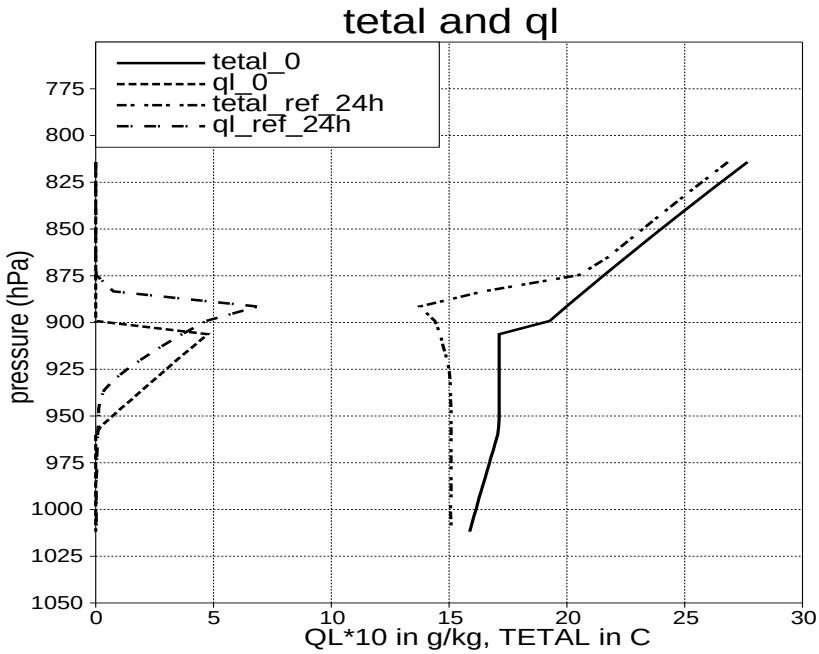

Figure 10: Vertical profiles of cloud condensate and liquid water potential temperature at initial time and at 24 hours forecast length for experiment 2.2 (REF) using high vertical resolution HIG (see text).

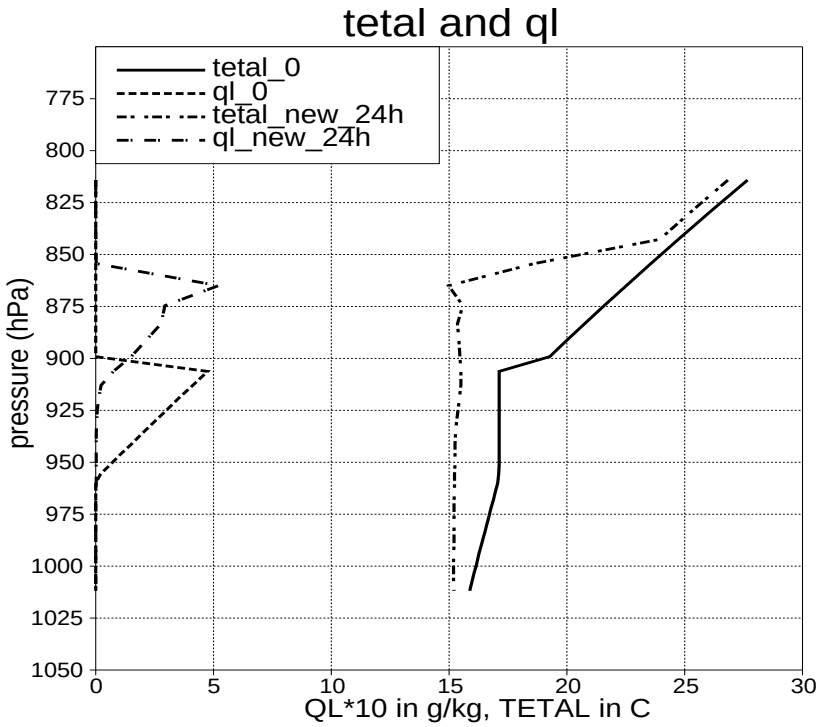

Figure 11: Vertical profiles of cloud condensate and liquid water potential temperature at initial time and at 24 hours forecast length in experiment 2.2 (NEW) using high vertical resolution HIG (see text).

4.2.3. Forcing from a strongly increasing pressure gradient

In this experiment the surface pressure gradient is further increased with time (20 m s^{-1} in 24 hours) becoming 25 m s^{-1}. Otherwise the conditions are the same as those for experiments 2.1 and 2.2. This experiment represents strongly non-stationary conditions with wind shear. It is seen that the entrainment rates are further increased due to the more intense mixing from shear production of turbulence (table 3b). As a qualitative comparison it is noted that the entrainment rate estimated by Nicholls and Leighton (1986) for a strong wind shear case was more than double of the average entrainment rate from the other five stratocumulus cases described in the paper. This serves of course only as a qualitative comparison. A large entrainment rate is associated with a significant downward heat flux. The effect of an increased downward heat flux is shown in the results of fig.12 valid for REF and in fig.13, valid for NEW. The Θ_l-profile of REF is now 'well mixed' apart from the small 'dip' near cloud top, mentioned for the previous experiment. The heating effect associated with a larger entrainment in NEW is clearly visible in Θ_l which is now generally higher compared to REF (lower relative humidity below cloud base). Also Θ_l increases up through the cloud, and the cloud liquid water of NEW is generally lower than seen in REF. These features are consistent with the slightly smaller precipitation amounts seen with NEW as compared to the previous experiment. The precipitation amounts of REF on the other hand show practically no change of the accumulated precipitation.

Table 3a:
Accumulated 24 hour precipitation for experiment 2.3 run for a strongly increasing pressure gradient. REF applies to unmodified scheme, NEW to the modified scheme. LOW, MED and HIG apply to a coarse, medium and a high vertical resolution respectively (see text)

model/res.	LOW	MED	HIG
REF	1.12	1.21	1.18
NEW	0.92	0.66	0.59

Table 3b:
Accumulated cloud top lift (hPa) for experiment 2.3 (see text) Numbers in brackets apply to the unmodified scheme. Results are shown for forecast lengths of 12, 24, 36 and 48 hours. LOW, MED and HIG apply to a coarse, medium and a high model resolution (res) respectively.

fclen/res.	LOW	MED	HIG
+12 h	+15 (0)	+30 (10)	+35 (15)
+24 h	+35 (15)	+55 (20)	+70 (35)
+36 h	+90 (50)	+110 (55)	+125 (70)
+48 h	+125 (70)	+140 (95)	+150 (105)

4.2.4. Effect of subsidence

This experiment (2.4) is different from the previous ones due to the application of a dynamical forcing in the form of a negative vertical velocity (subsidence) fixed in time.

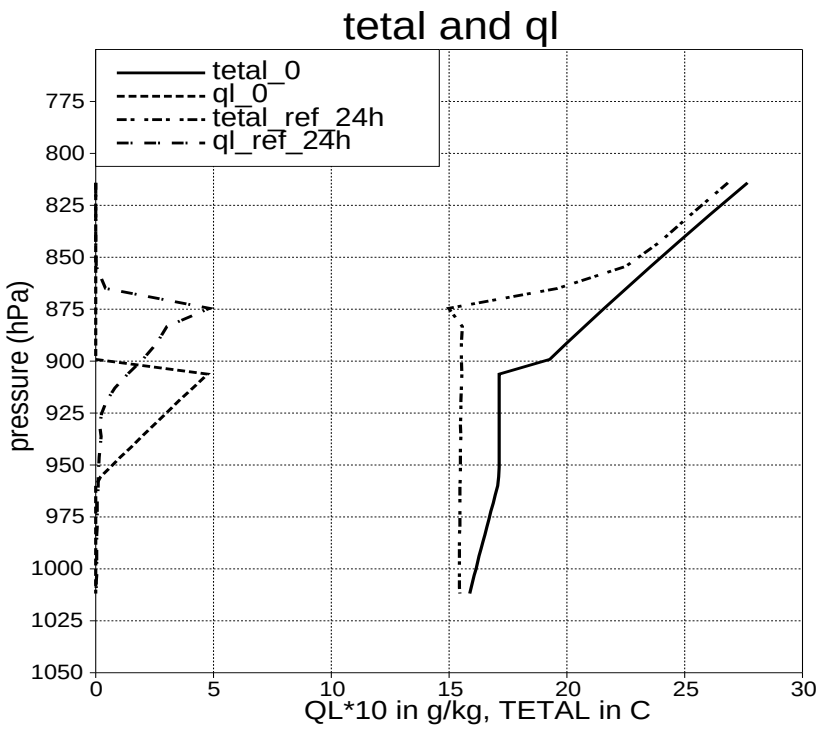

Figure 12: Vertical profiles of cloud condensate and liquid water potential temperature at initial time and at 24 hours forecast length for experiment 2.3 (REF) using the high vertical resolution HIG (see text)

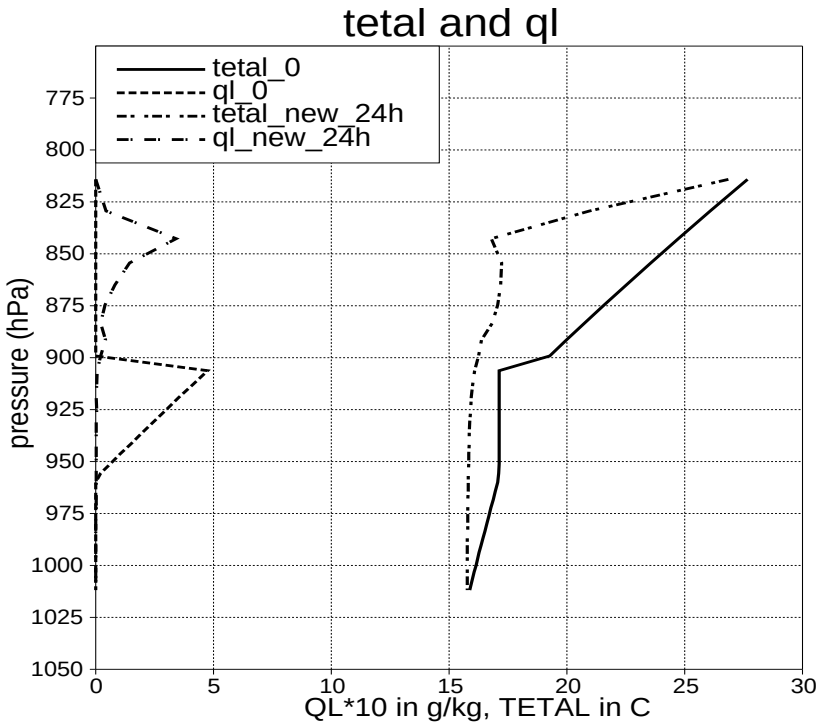

Figure 13: Vertical profiles of cloud condensate and liquid water potential temperature at initial time and at 24 hours forecast length for experiment 2.3 (NEW) using the high vertical resolution HIG (see text)

The velocity varies linearly with height and reaches 0.5 cm s^{-1} at a height of 1000 m. Above this level it is assumed constant with increasing height. It is emphasized that the forcing operates such as to advect both temperature and humidity in the vertical. Also the heating due to compression is necessarily included. In addition, the moderate tendency of the surface pressure gradient corresponds to experiment 2.2.

The results of the accumulated precipitations and entrainment (comparable to the results of the previous experiments) are shown in tables 4a and 4b. The ** (double-star) means that the cloud no longer exists, implying that no cloud top displacement can be determined. The high resolution profiles at +24 hours are shown in fig.14 (REF) and in fig.15 (NEW)

An examination of the role of different processes shows that for both REF and NEW the effects of subsidence are very important and in fact decisive for the cloud evolution. As a consequence of the advections near cloud top, the vertical movement is approximately zero as opposed to previous figures. In this case the subsidence counteracts the effects of entrainment such that the cloud top is quasi-stationary. At +24 hours a slight lowering of the cloud top has occured in NEW at medium and high resolution. The tendency for drying and heating from vertical advection leads to marked reductions of the 24-hour accumulated precipitations in both REF and NEW (see table 4a). In this experiment the precipitations of the new version are only marginally smaller than the counterparts of REF. It turns out that for both model versions the cloud disappears relatively independent of model resolution. All clouds are gone after 36 hours in all model versions. The cloud cover decay period (from 100 % to 0%) is 1 to 1.5 hours. It turns out that the sum of dynamical heating at cloud top plus heating due to condensation and turbulence becomes larger than the counteracting cooling due to radiation. In addition, the vertical advection of moisture acts as a drying. The combined effect is to destroy the cloud. From fig.15 it is seen that the cloud is shrinking 'from above and from below'.

Table 4a:
Accumulated 24 hour precipitation for experiment 2.4 (see text). REF applies to unmodified scheme, NEW to the modified scheme. LOW, MED and HIG apply to a coarse, medium and a high vertical resolution, respectively.

model/res.	LOW	MED	HIG
REF	0.43	0.49	0.40
NEW	0.39	0.40	0.27

Table 4b:
Accumulated cloud top lift (hPa) for experiment 2.4 (see text). Numbers in brackets apply to the unmodified scheme. Results are shown for forecast lengths of 12, 24, 36 and 48 hours. LOW, MED and HIG apply to a coarse, medium and a high model resolution (res) respectively.

fclen/res.	LOW	MED	HIG
+12 h	0 (0)	0 (0)	+5 (0)
+24 h	0 (0)	-10 (0)	-5 (0)
+36 h	** (**)	** (**)	** (**)
+48 h	** (**)	** (**)	** (**)

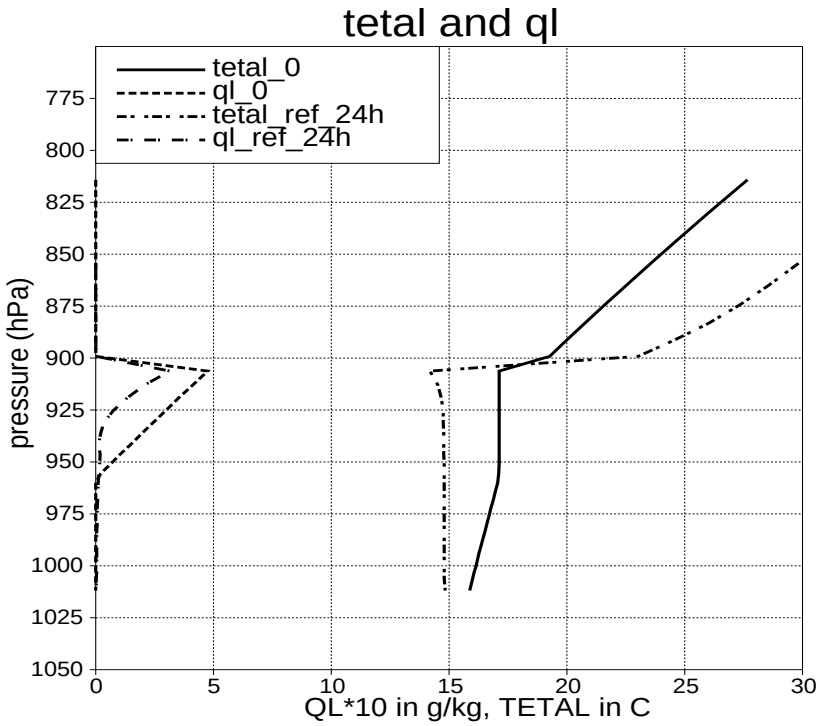

Figure 14: Vertical profiles of cloud condensate and liquid water potential temperature at initial time and at 24 hours forecast length for experiment 2.4 (REF) using the high vertical resolution HIG.

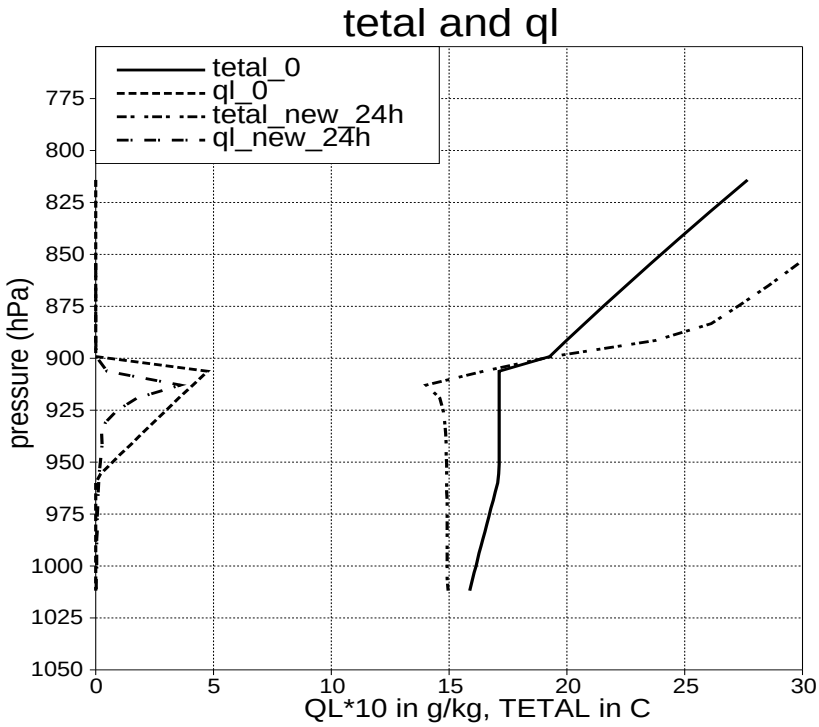

Figure 15: Vertical profiles of cloud condensate and liquid water potential temperature at initial time and at 24 hours forecast length for experiment 2.4 (NEW) using the high vertical resolution HIG

4.2.5. Effect of surface fluxes

In this experiment (2.5) the subsidence velocity is set to zero, but the surface fluxes are different from zero. Otherwise the conditions are the same as for the previous experiment (2.4). First the latent surface heat flux is set to 50 W m^{-2} (constant). The effect on precipitation and cloud top evolution are seen in tables 5a and 5b. The additional moisture source corresponding to 2.1 mm day^{-1} gives rise to more precipitation (table 5a compared to table 2a) but also more entrainment (table 5b versus table 2b). It is still apparent that the entrainment is larger while the precipitation is smaller in NEW compared with REF. It is seen that the low resolution results no longer suffer from smaller entrainment compared with high resolution results. It also turns out that the cloud and sub-cloud layers tend to be well mixed (no decoupling). This is consistent with the finding in various investigations that increased surface fluxes tends to promote a well mixed boundary layer (cloud +sub-cloud layers).

Finally, the effect of increasing the upward sensible heat flux is investigated while keeping a zero surface latent heat flux. One may expect that the cloud will be destroyed after some time due to a heating effect from below. This is confirmed. The surface heat flux, however, requires to be as high as 125 W m^{-2}. The time required for cloud dissipation is roughly the same in both model versions. The last two hours of a 2 day simulation is completely cloud free. Application of larger upward heat fluxes will dissipate the cloud earlier. It is noted that during the simulation the cloud becomes deeper and deeper, and therefore the efficiency of the heating with a constant flux becomes smaller.

Table 5a :
Accumulated 24 hour precipitation for experiment 2.5. REF applies to unmodified scheme , NEW to the modified scheme. LOW, MED and HIG apply to a coarse, medium and a high vertical resolution respectively (see text)

model/res.	LOW	MED	HIG
REF	1.30	1.50	1.55
NEW	1.02	0.98	1.14

Table 5b:
Accumulated cloud top lift (hPa) for experiment 2.5. Numbers in brackets apply to the unmodified scheme. Results are shown for forecast lengths of 12, 24, 36 and 48 hours. LOW, MED and HIG apply to a coarse, medium and a high model resolution (res), respectively.

fclen/res.	LOW	MED	HIG
+12 h	+50 (35)	+30 (10)	+25 (15)
+24 h	+70 (35)	+70 (20)	+55 (30)
+36 h	+110 (35)	+95 (35)	+85 (45)
+48 h	+125 (50)	+125 (45)	+125 (60)

4.3. Case 3

This case concerns very stable conditions at cloud top according to the Mason-McVean criterion ($K_{ctei} = 0.10$). The intial conditions of temperature and specific humidity are again constant above cloud top initially but differ from case 1 according to the value chosen for K_{ctei}. The initial profiles of cloud water (dashed lines) and liquid water potential temperature (solid lines) are shown in fig.16. The initial conditions depend to some extent on the chosen vertical discretization as mentioned also for case 2. Most experiments below may be compared to a corresponding experiment studied in case 2.

4.3.1. Forcing from a weak constant pressure gradient

The results from this experiment (3.1) are to be compared qualitatively with experiment 2.1. This means that this case is run for a constant weak surface geostrophic wind (5m s^{-1}) and zero surface fluxes, but with a strong inversion associated with the small value of K_{ctei}. The results for accumulated precipitation and cloud top displacement are given in tables 6a and 6b respectively. The evolution over 24 hours of Θ_l and q_l are shown in fig.16 (REF) and fig.17 (NEW).

It is seen that the differences between the results of REF and NEW are more marked than for experiment 2.1. Table 6a reveals that the reduction of the accumulated precipitation in version NEW is more pronounced (e.g., 0.41 mm versus 1.25 mm for 'HIG'). Table 6b shows that the cloud top height is completely fixed in time for REF (except at +48h in the high resolution run). The new version is still able to lift the cloud top, but mainly at medium and high resolution. This experimental situation is most crucial for the reference version. With practically no wind shear and a very stable stratification, according to the current version of the turbulence scheme, there is no significant fluxes due to turbulence across the inversion. Since the default convection scheme does not either supply the adequate transports the cloud top is 'locked'. It is subject to cooling due to radiation and generation of more liquid water. Precipitation release also becomes significant. These features are strongly apparent in fig.16 (to be compared with fig.8) For the revised scheme fig.17 may be compared with fig.9 for the unstable case. A distinct decoupling near cloud base is visible at +24 hours and the profile of Θ_l resembles that shown in fig.9. Although the entrainment has been reduced it is still significant in NEW. This is achieved by the non-local character of the mixing described at cloud top involving buoyant air parcels. This treatment is qualitatively linked to vertical velocity variance near cloud top which is regarded to be quite important for the computation of W_e (Nicholls, 1984). A quantitative assessment of the quality of computations with the new scheme is however difficult to make (see section 5).

Table 6a :
Accumulated 24 hour precipitation for experiment 3.1. REF applies to unmodified scheme, NEW to the modified scheme. LOW, MED and HIG apply to a coarse, medium and a high vertical resolution respectively (see text)

model/res.	LOW	MED	HIG
REF	1.23	1.30	1.25
NEW	0.68	0.63	0.41

Table 6b:
Accumulated cloud top lift (hPa) for experiment 3.1 (see text) Numbers in brackets apply to the unmodified scheme. Results are shown for forecast lengths of 12, 24, 36 and 48 hours. LOW, MED and HIG apply to a coarse, medium and a high model resolution (res) respectively.

fclen/res.	LOW	MED	HIG
+12 h	+0 (0)	+0 (0)	+10 (0)
+24 h	+15 (0)	+10 (0)	+25 (0)
+36 h	+15 (0)	+25 (0)	+35 (0)
+48 h	+15 (0)	+35 (0)	+45 (10)

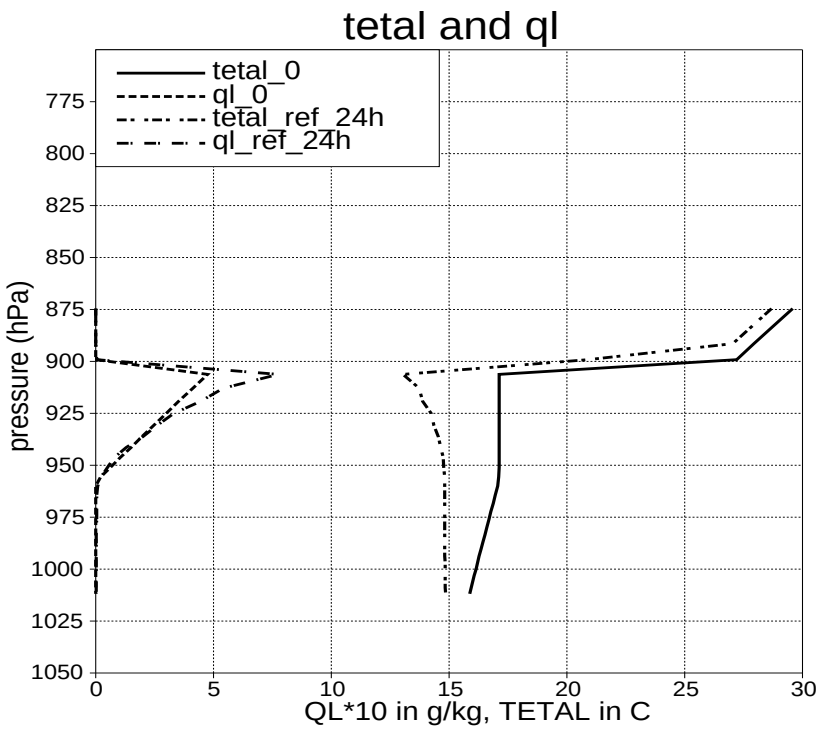

Figure 16: Vertical profiles of cloud condensate and liquid water potential temperature at initial time and at 24 hours forecast length for experiment 3.1 (REF) using the high vertical resolution HIG

4.3.2. Forcing from a moderately increasing pressure gradient

The experimental conditions are comparable to those of experiment 2.2 (moderately increasing geostrophic wind to 15 m s^{-1} after 24 hours). The corresponding results for precipitation and cloud top movement are shown in tables 7a-b. The profiles of Θ_l and q_l are shown in fig.18 and fig.19.

The results of REF are very similar to the corresponding ones of fig.10. The new scheme produces slightly more entrainment compared to experiment 3.1, but less en-

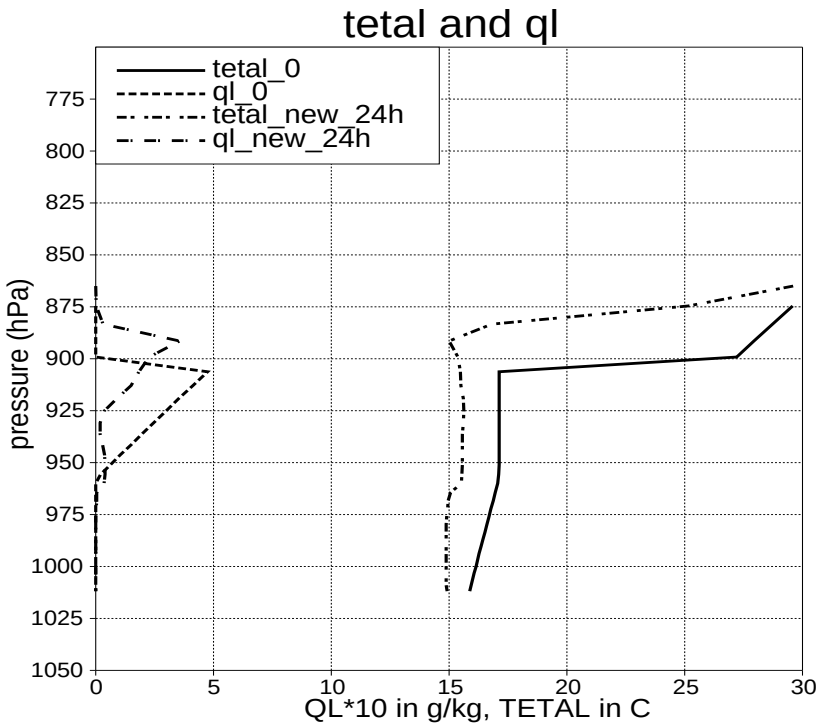

Figure 17: Vertical profiles of cloud condensate and liquid water potential temperature at initial time and at 24 hours forecast length for experiment 3.1 (NEW) using a high vertical resolution HIG.

Table 7a:
Accumulated 24 hour precipitation for experiment 3.2 run with forcing from a moderately increasing surface pressure gradient. REF applies to unmodified scheme , NEW to the modified scheme. LOW, MED and HIG apply to a coarse, medium and a high vertical resolution (see text)

model/res.	LOW	MED	HIG
REF	1.30	1.46	1.42
NEW	0.68	0.69	0.70

Table 7b:
Accumulated cloud top lift (hPa) for experiment 3.2. Numbers in brackets apply to the unmodified scheme. Results are shown for forecast lengths of 12, 24, 36 and 48 hours. LOW, MED and HIG apply to a coarse, medium and a high model resolution (res) respectively.

fclen/res.	LOW	MED	HIG
+12 h	+0 (0)	+0 (0)	+5 (0)
+24 h	+15 (0)	+20 (0)	+25 (0)
+36 h	+15 (0)	+45 (0)	+45 (0)
+48 h	+35 (0)	+55 (10)	+65 (15)

trainment compared to to the 'unstable' counterpart (experiment 2.2). The increase of Θ_l near cloud base and decrease towards the top at +24 hours is more pronounced in this case. The realism of this feature is difficult to estimate.

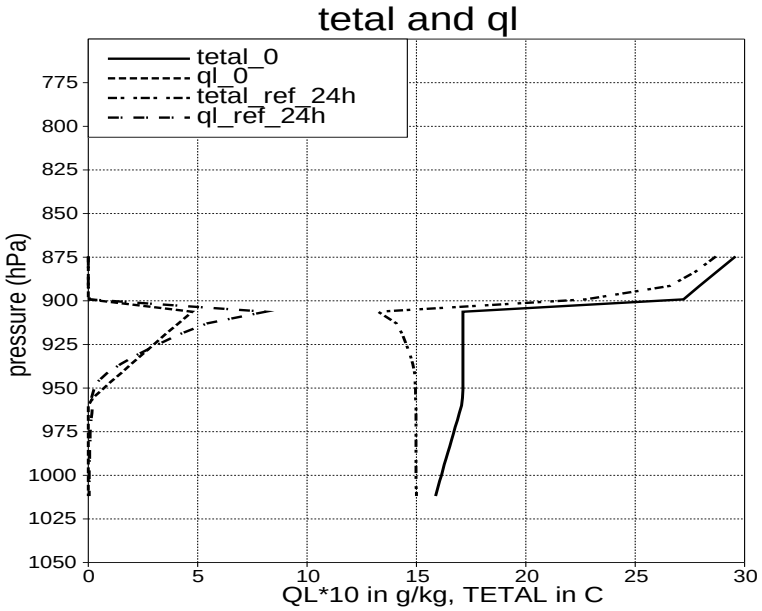

Figure 18: Vertical profiles of cloud condensate and liquid water potential temperature at initial time and at 24 hours forecast length for experiment 3.2 (REF) using the high vertical resolution HIG.

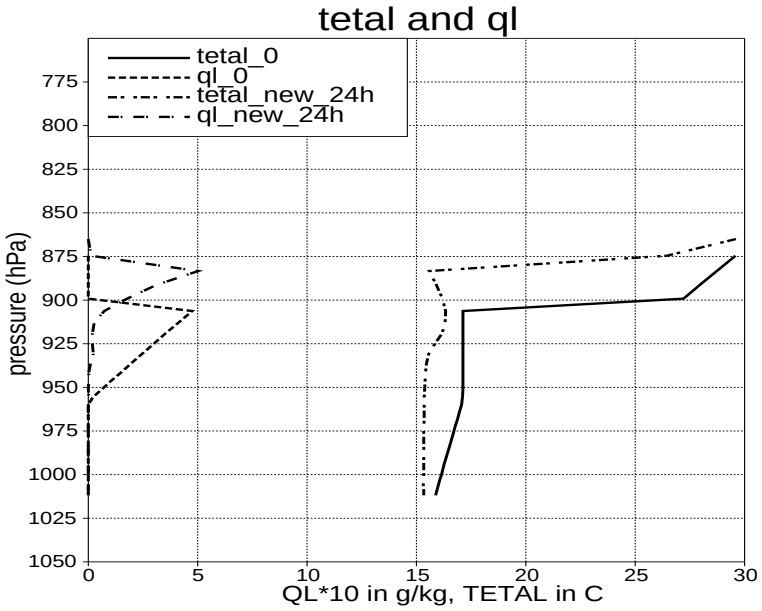

Figure 19: Vertical profiles of cloud condensate and liquid water potential temperature at initial time and at 24 hours forecast length for experiment 3.2 (NEW) using the high vertical resolution HIG.

4.3.3. Forcing from a strongly increasing pressure gradient

The results of this experiment (3.3) differ quantitatively from the corresponding experiment 2.3 in Case 2. It is emphasized that it is a case of strong wind shear. The geostrophic wind increases by 20 m s^{-1} per day starting at 5 m s^{-1}. It is seen from fig.21 (NEW) that the maximum cloud water occurs significantly below cloud top. It is apparent from the Θ_l-profile that the cloud has mixed to higher levels as revealed by the gradual increase of Θ_l compared to the original profile (fig.21). This vertical distribution is opposed to the idealized distribution in mixed layer models with a quasi-linear increase of liquid water up to the cloud top.

Table 8a :
Accumulated 24 hour precipitation for experiment 3.3 run with a strongly increasing surface pressure gradient. REF applies to unmodified scheme, NEW to the modified scheme. LOW, MED and HIG apply to a coarse, medium and a high vertical resolution respectively (see text)

model/res.	LOW	MED	HIG
REF	1.29	1.49	1.41
NEW	0.64	0.58	0.46

Table 8b:
Accumulated cloud top lift (hPa) for experiment 3.3. Numbers in brackets apply to the unmodified scheme. Results are shown for forecast lengths of 12, 24, 36 and 48 hours. LOW, MED and HIG apply to a coarse, medium and a high model resolution (res), respectively.

fclen/res.	LOW	MED	HIG
+12 h	+0 (0)	+10 (0)	+15 (0)
+24 h	+15 (0)	+35 (0)	+35 (0)
+36 h	+35 (15)	+60 (20)	+70* (25)
+48 h	+70 (35)	+95 (60)	+105 (70)

A qualitative comparison with the strong wind shear case studied by Nicholls and Leighton (1986), and by Duynkerke and Driedonks (1988), is again of some relevance because of the large geostrophic wind. This case from 15 December 1982 is characterized by wind speeds up to more than 30 m s^{-1} in the boundary layer. These authors find that a substantial downward (negative) heat- and buoyancy flux extends from cloud top and towards the surface. At the same time the humidity flux is upwards. The entrainment of dry warm air leads to remarkably low values of cloud water in the upper part of the cloud. The maximum cloud water amount (0.3 g_{water} kg^{-1}) occurs about 30 % down into the cloud. These features are obviously similar to the results from fig.21. However, it should be born in mind that the comparison can only be qualitative. An investigation of the results of NEW reveals that the heat flux is downward while the moisture flux is upward. The latter is seen from the fact that the total specific humidity decreases with time close to the surface, from about 9.5 g_{water} kg^{-1} to 8.2 g_{water} kg^{-1} after 24 hours.

Table 8a shows that the reduction in accumulated precipitation is substantial when using the revised model version. Also entrainment is still substantially higher with NEW but the effect of wind shear now allows for some entrainment (table 8b). The * (star)

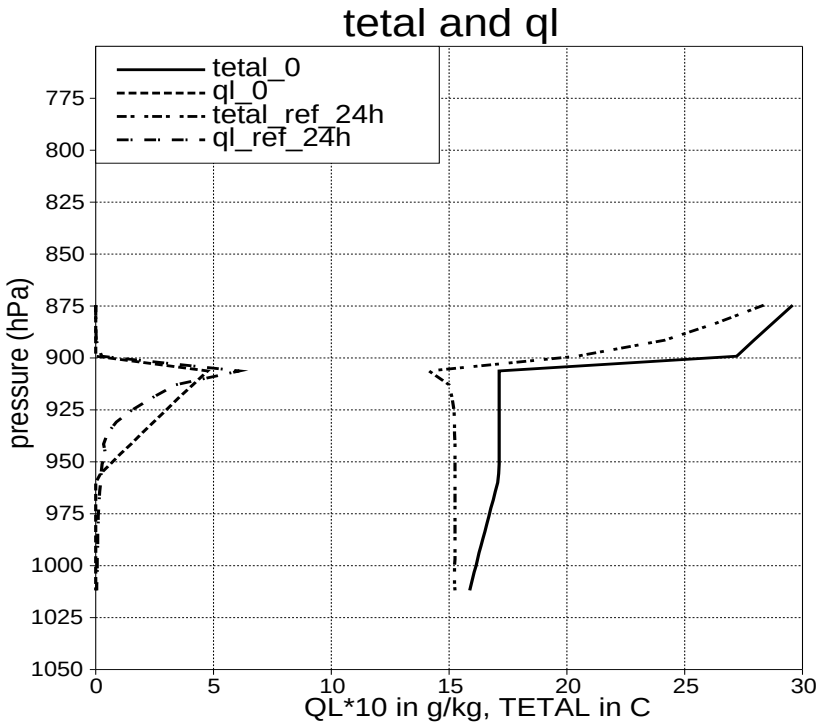

Figure 20: Vertical profiles of cloud condensate and liquid water potential temperature at initial time and at 24 hours forecast length for experiment 3.3 (REF) using the high vertical resolution HIG.

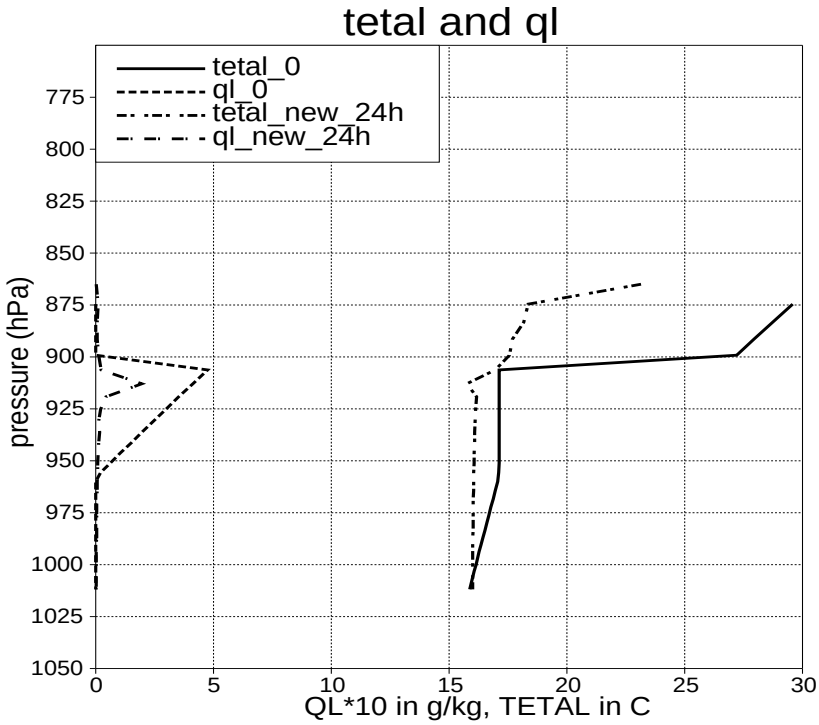

Figure 21: Vertical profiles of cloud condensate and liquid water potential temperature at initial time and at 24 hours forecast length for experiment 3.3 (NEW) using the high vertical resolution HIG.

in the table is valid for high resolution at +36 hours. It signifies that the cloud cover is broken (77 %). Fig.20, valid for REF, shows that cloud water is reduced at cloud top compared to the preceeding experiments (3.1 and 3.2), but at +24 hours there are not signs of significant entrainment.

4.3.4. Effect of subsidence

The experimental conditions in experiment 3.4 are comparable to those of 2.4, that is, a maximum subsidence velocity of 0.5 cm s^{-1} at heights no less than 1000 m is used (linear decrease towards surface). Also the surface fluxes are forced to remain zero.

As for experiment 2.4 there is a clear manifestation of subsidence. The precipitation amounts are small and similar for model versions (table 9a). It turns out that the evolution of cloud cover is more complicated in this experiment (see table 9b). It is seen that the cloud dissipation (**) happens at different times. Also partial cloud breakup (*) is involved. The quicker dissipation during the first 12 hours for the coarse resolution runs may be related to the actual position of the model levels, e.g. the specific cloud water at the uppermost cloud level is slightly lower initially at coarse resolution (LOW) due to a lower position of that level. For the new model version cloud cover is also broken at +12 hours for medium and high resolution. For the medium resolution a complete dissipation of the clouds has taken place after +17 hours. The cloud disipates later (at 31 - 32 hours) with the reference version at medium resolution. The cloud evolution process is characterized by cloud 'shrinking' which has been seen also for the previous experiment with subsidence. This is reflected in fig.22 and fig.23 showing the high resolution profiles of Θ_l and q_l for REF and NEW, respectively. Also the downward movement of cloud top due to subsidence is seen from the negative numbers appearing in table 9b. A special situation occurs in the high resolution run of the new version. The cloud almost dissipates during the first 12 hours due to the combined efffect of mixing and subsidence, but is later reestablished at a lower level where radiative cooling leads to cloud formation. Later, between 33 hours and 34 hours, the cloud finally dissipates. It turns out that subsidence and heating due to turbulent mixing closer to the surface finally dominates over cooling due to radiation at these later stages of the simulation. At +24 hours the specific cloud water in the cloud is exceptionally higher with NEW compared to REF. This is also reflected in the special situation of slightly higher precipitation amount (0.31 versus 0.22) in table 9a. All experiments result in cloud dissipation no later than about 34 hours into the simulation.

Table 9a :
Accumulated 24 hour precipitation for experiment 3.4 REF applies to unmodified scheme , NEW to the modified scheme . LOW, MED and HIG apply to a coarse, medium and high vertical resolution respectively (see text)

model/res.	LOW	MED	HIG
REF	0.03	0.22	0.22
NEW	0.02	0.12	0.31

Table 9b:
Accumulated cloud top lift for experiment 3.4. Numbers in brackets apply to the unmodified scheme. Results are shown for forecast lengths of 12, 24, 36 and 48 hours. LOW, MED and HIG apply to a coarse, medium and a high model resolution (res) respectively (see text).

fclen/res.	LOW	MED	HIG
+12 h	** (**)	-25* (-10)	-10* (-5)
+24 h	** (**)	** (-20)	-30 (-15)
+36 h	** (**)	** (**)	** (**)
+48 h	** (**)	** (**)	** (**)

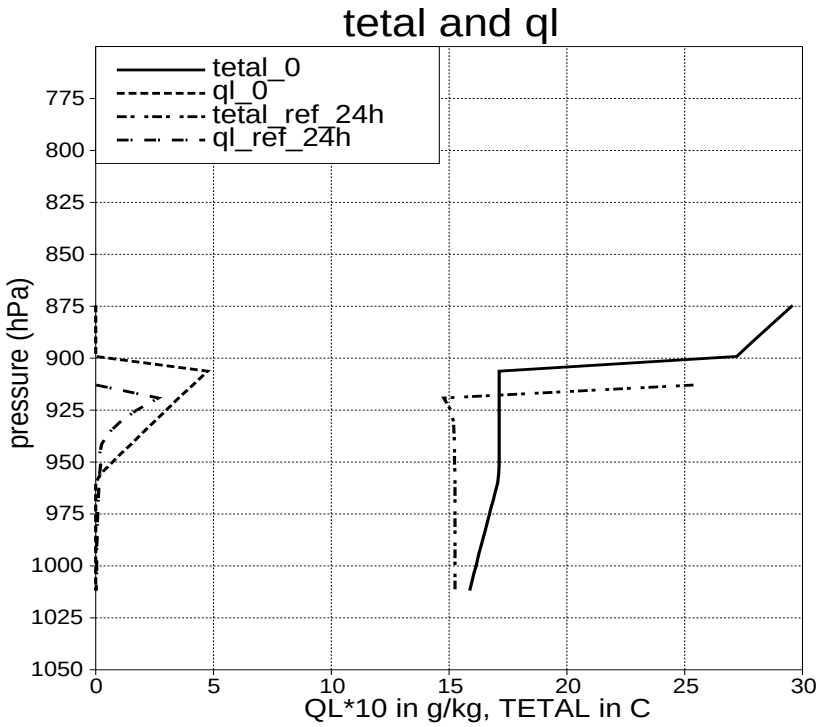

Figure 22: Vertical profiles of cloud condensate and liquid water potential temperature at initial time and at 24 hours forecast length in experiment 3.4 (REF) using the high vertical resolution HIG.

4.3.5. Impact of surface fluxes

Also for the stable case the effect of surface fluxes is investigated. First, the latent heat flux is increased to 50 W m^{-2} directed upwards. The forcing is similar to that of experiment 2.5. It is seen from table 10a that the 24 hour accumulated precipitations are increased compared to the previous experiments consistent with the additional moisture supply from the surface. However the precipitation increase is most significant in the reference version. The precipitation differences are quite significant .e.g., 1.83 mm versus 0.79 mm in the high resolution run. The movement of cloud top as displayed in table 10b is interesting. It is seen that sensitivity to model resolution is quite modest as compared to most other experiments. The differences between the entrainments of NEW and REF are substantial.

Secondly, the surface sensible heat flux is increased until the cloud dissipates during the 48 hour period. The surface latent heat flux is set to zero in these experiments. It turns out that a modest sensible heat flux is required as compared to the unstable case (experiment 2.5). For REF a heat flux of 55 W m^{-2} is required to dissipate the cloud. This is to be compared with a value of 125 W $\cdot$ m^{-2} in experiment 2.5. This difference can be explained qualitatively by a significantly larger entrainment rate in 2.5. As a consequence a thicker layer has to be heated in order to dissipate the cloud. The same effect can probably explain that a slightly higher sensible heat flux is required (65 W m^{-2}) to dissipate the cloud with the new model version.

In fig.24 is shown the vertical maximum cloud cover evolution over 20 hours (240 time

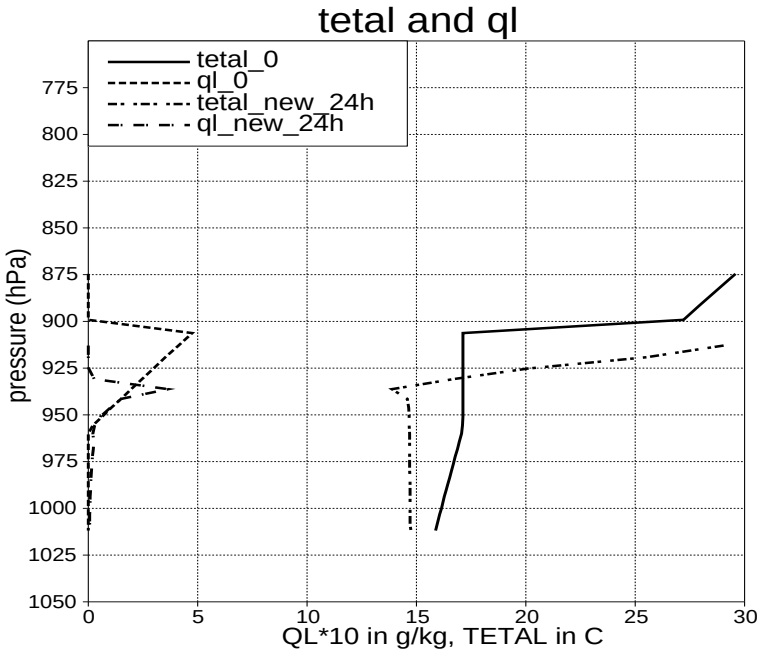

Figure 23: Vertical profiles of cloud condensate and liquid water potential temperature at initial time and at 24 hours forecast length for experiment 3.4 (NEW) using the high vertical resolution HIG.

steps) in an experiment where the effect of combining different forcings is investigated. Both the surface sensible and latent heat fluxes are kept fixed at 100 W m^{-2}, and a subsidence profile is imposed in the same way as in experiments 2.4 and 3.4. It is seen that the cloud cover evolutions of REF and NEW are quite different. The combined effect of the surface fluxes and the heating due to subsidence leads to these different results with the two model versions. The reference simulation keeps the cloud solid until about 12 $\frac{1}{2}$ hours integration and a rapid dissipation happens during the subsequent hour. The new scheme predicts low cloud amount after about 3 hours . After $7\frac{1}{2}$ hours integration time the cloud cover is reestablished as also seen in experiment 3.4. Again the cloud dissipates quickly between 13 and 14 hours forecast length which is almost at the same time as seen with REF. This illustrates the complex cloud prediction problem when several significant processes are involved. More experiments using fixed upward surface fluxes of sensible and latent heat in the interval [0,200] W m^{-2} indicate that periods with fractional cloudiness, e.g., less that 50 % occurs more often with the new formulation than with the reference one. This is considered to reflect the larger entrainment of dry and warm air with the revised scheme.

Table 10a:
Accumulated 24 hour precipitation for experiment 3.5 (see text). REF applies to unmodified scheme , NEW to the modified scheme. LOW, MED and HIG apply to a coarse, medium and a high vertical resolution respectively.

model/res.	LOW	MED	HIG
REF	1.69	1.85	1.83
NEW	0.71	0.90	0.79

Table 10b:
Accumulated cloud top lift (hPa) for experiment 3.5 (see text). Numbers in brackets apply to the unmodified scheme. Results are shown for forecast lengths of 12, 24, 36 and 48 hours. LOW, MED and HIG apply to a coarse, medium and a high model resolution (res) respectively.

fclen/res.	LOW	MED	HIG
+12 h	15 (0)	+10 (0)	+15 (0)
+24 h	+35 (0)	+35 (0)	+35 (5)
+36 h	+50 (0)	+55 (0)	+55 (10)
+48 h	+70 (15)	+70 (10)	+85 (15)

4.4. Sensitivity to entrainment parameter

It is relevant to ask about the sensitivity of the results with the new scheme as regards the choice of the value of the entrainment parameter K_* which is a key parameter in the scheme. The results presented so far with the new scheme have all used a value $K_* = 0.25$. It is difficult to estimate the uncertainty involved with the choice of this value, that is, whether a higher or a lower value will provide improved results. Currently, the parameter must to some extent be regarded as a tuning parameter of the scheme.

We may, as a rough estimate, compare the simulated entrainment rates of the present

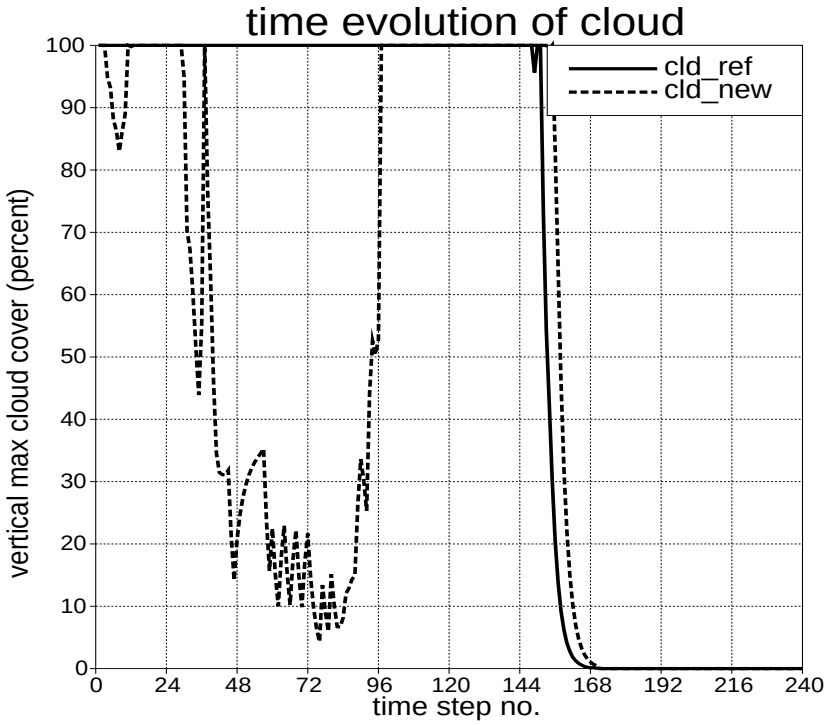

Figure 24: Evolution of maximum cloud cover in REF and NEW for the case of a maximum subsidence velocity of 0.005 m/s at 1000 m, a geostrophic wind of 5 m/s and surface fluxes of sensible and latent heat= 100 W/m2 using a standard entrainment coefficient (0.25) in NEW.

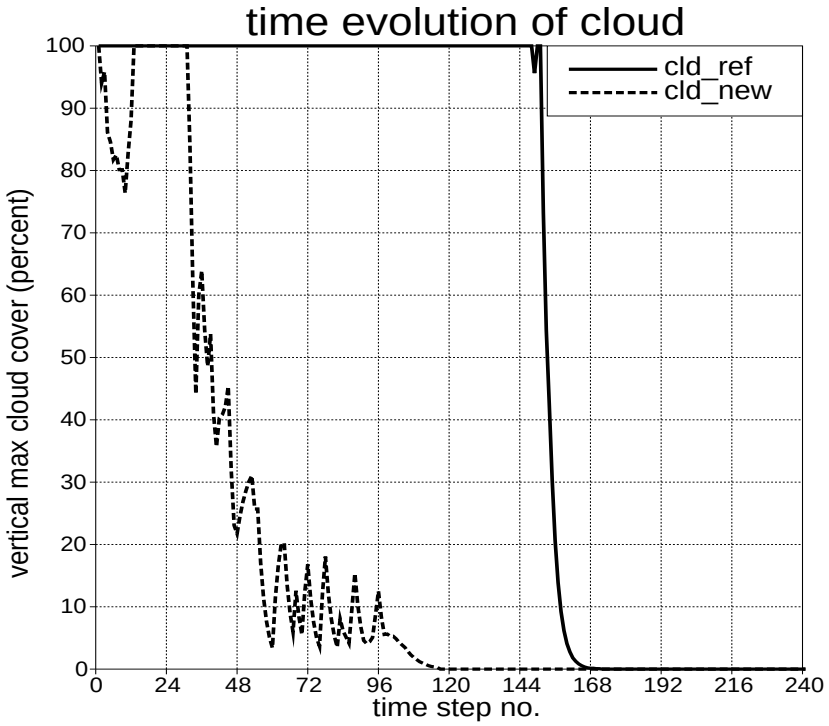

Figure 25: Evolution of maximum cloud cover in REF and NEW for the case of a maximum subsidence velocity of 0.005 m/s at 1000 m, a geostrophic wind of 5 m/s and surface fluxes of sensible and latent heat = 100 W/m2 using an entrainment coefficient of 0.35 in NEW.

idealized experiments, using zero fluxes, with those deduced by Nicholls and Leighton in 1986 for stratocumulus around the British Isles (their table 7). It is emphasized that 4 out of these 5 cases are classified as 'decoupled', which provides some similarity to the present experiments using zero surface fluxes. The average deduced W_e from this table provides a value of 0.49cm s^{-1}. Leaving out the case which is not decoupled, does not significantly change this value. The measurements were mostly done during daytime with solar heating effects which favours relatively low entrainment rates.

A simple estimate of the entrainment rate (no solar heating) from the present idealized experiments, using the new model version at a high vertical resolution, gives an average entrainment rate of 0.38 cm s^{-1}. This computation involves only the experiments with zero surface fluxes, and the strong wind experiments (2.3 and 3.3) are left out.

A comparison between these values can at most indicate that the present choice of the value for K_* is probably not too large. This is further supported by the results of the ASTEX simulations, but here only a modest increase of the simulated entrainment will be in accordance with the estimated values from the observational study. Experimentation shows that entrainment rates does increase significantly if K_* is increased. However, a modest increase of the parameter, e.g., to a value of 0.35, seems to produce results consistent with the constraints defined by the previous discussion. The impact of using K_* =0.35 instead of 0.25 for the experiment, with combined forcing from surface (100 W m^{-2}) and from subsidence (see fig.24), is illustrated in fig.25. Interestingly, the cloud cover does not reestablish between 8 and 13 hours of simulation time. Instead, the cloud dissipates completely around 9 hours into the forecast.

5. Discussion and conclusions

This work has been devoted to the problem of modelling the time evolution of clouds capped by a stable layer. The numerical study has been motivated partly by a wish to explain and cure a deficiency in the precipitation forecasts with the HIRLAM forecasting system, which tends to predict small precipitation amounts with a too high frequency compared with observations.

A basic hypothesis has been made to explain the excessive occurrence of small precipitation intensities. It has been postulated that too small fluxes of heat and moisture on top of low troposheric clouds poses a key problem, which is reflected also in a too small entrainment of air on the cloud tops. As a consequence, the downward sensible heat transport does not compensate enough for the cooling due to radiation flux divergence, leading to excessive cloud water and precipitation release. Also the profile of liquid water potential temperature (Θ_l) tends to become unrealistic with a too large temperature decrease near cloud top.

In order to test the ideas connected to the basic hypothesis, an extension has been made to the model formulation of the vertical heat and moisture transports on the top of clouds capped by a stable layer. This formulation expressing the effect of shallow convection partially penetrating the transition to the stable layer is based on physical reasoning and has the potential to increase the heat and moisture exchange between the cloudy layer and the overlying atmosphere, compared with the default version of the physical parameterizations. Currently, the revised scheme as described in section 3,

is also used to describe the effect of overshooting eddies in situations with mid-level or deep convection.

The tests with the new model version and the default version have clearly supported the basic hypothesis that too little entrainment of dry air from the stable layer above stratocumulus plays a significant role in the development of an excess frequency of small precipitation amounts. The simulations show that the new scheme is capable of producing increased entrainment of the air above cloud top.

Large precipitation amounts, e.g., more than 10 mm in 12 hours are not likely to be reduced by the new formulation. In fact, during periods of stratocumulus, more moisture is transferred through the cloud top to the atmosphere above. This additional moisture is available for stronger precipitation events later, involving deep layers in the troposphere.

Preliminary 3-dimensional runs with the HIRLAM forecasting system support the precipitation characteristics mentioned above for the new model version.

The results indicate that the precipitation amounts with the reference version are, on average, insensitive or marginally increasing with higher vertical resolution. The precipitation with the revised model appears to be insensitive or marginally decreasing with higher vertical resolution. It should be born in mind that this feature may be somewhat modified in a 3-dimensional model where a mutual interaction between physics and dynamics comes into play.

The estimates of entrainment rates in observational studies are associated with a rather high relative error margin. This adds to the general problem of developing realistic parameterizations of the moisture and energy fluxes near the top of stratocumulus.

The model simulated entrainment for the ASTEX case is quite realistic for the new model version when compared with the entrainment velocity determined in the observational study. Qualitative comparisons with entrainment rates determined in other observational studies, e.g., by Nicholls and Leighton (1986) in a study of stratocumulus around the British Isles, suggest that none of the tested model resolutions produce excessive entrainment. The vertical resolution tested covers a range between 7 and 25 levels in the lowest kilometre of the atmosphere. The experiments exhibit some sensitivity to model resolution, in particular in weak wind situations with zero (small) surface fluxes of sensible and latent heat. This feature associated with small surface fluxes may result in too persistent boundary layer clouds in a 3-dimensional model using a coarse vertical resolution, especially if the analysis scheme to determine the initial conditions is very conservative with respect to boundary layer structure. Under the same conditions, a high resolution of the new model version will in many situations describe significant changes in the position of the cloud, which is probably advantageous when cloud persistency is to be avoided. A reduction of the entrainment rate with a coarse resolution has not been obvious when the surface fluxes are moderate or high.

Generally the results of the model simulations in high resolution do not appear to reveal any special problems. It is noteworthy that cloud decoupling which is claimed to be very common under conditions of small surface fluxes (Nicholls and Leighton 1986) has been simulated in experiments with the new scheme under the conditions of zero surface

fluxes. It is, however difficult to estimate the realism of the vertical position of the decoupling and the actual magnitude of the phenomenon. In the present simulations decoupling occurs close to cloud base.

The entrainment instability leading to cloud breakup has not been simulated in case 2 where instability should occur according to the Mason-MacVean criterion. One possible reason for this might be the fact that only 1-dimensional experiments have been made whereas the study of MacVean (1993) is made with a 2-dimensional very high resolution large-eddy simulation model. Most studies in the litterature dealing with entrainment instability appear to make use of large-eddy simulation models.

It is not clear whether 1-dimensional models should be able to produce cloud dissipation beyond the instability limit defined by Mason & MacVean. It is noted that some 1-dimensional studies e.g., Chen and Cotton (1983) have focused on increased entrainment rates as a sign of entrainment instability, and not on the actual cloud dissipation. Furthermore, some experiments investigating entrainment have been carried out using artificial initial conditions, e.g., rapid cooling at cloud top. The study of MacVean (1993) has the more ambitious goal to actually demonstrate cloud dissipation under realistic experimental conditions.

The specification of initial conditions is an important issue in MacVean's large-eddy simulations. For example, MacVean pays special attention to the initial conditions above cloud top such as to enable that the stability parameter K_{ctei} does not change substantially during the short time of the experiment. Similar precautions have not been made in the present study. More experimentation is needed to further clarify the role of initial conditions. However, even if the instability criterion of MacVean is fully valid and leads to cloud dissipation, it is clear that the regime where this mechanism operates is greatly reduced, compared to the original criterion by Randall and Deardorff. Therefore, it seems that cloud top entrainment instability, although of theoretical interest, is of limited significance.

The present study indicates that the time evolution of stratocumulus is highly complex and involves cloud modifications on a wide range of time scales from less than one hour to several days. Forecasting the details of a cloud evolution seems to be generally a big and fascinating challenge. This is indicated by the examples presented for case 3, where the partitioning between the magnitude of forcing from different physical processes varies a lot as a function of time. The complex interaction between different processes, e.g., subsidence, radiation, turbulence, surface processes and condensation, is interesting. It is noted that the present study has not included the effect of solar radiation which is likely to be very important in a number of cases.

The experience from the present study is in line with the study of Weaver and Pearson (1990) emphasizing the role of subsidence as an effective mechanism for cloud dissipation. Also the study of Price (1999) emphasizing the importance of sensible heat flux from the surface and of strong wind shear, is qualitatively consistent with the results of the present study.

As already mentioned, the current turbulence scheme is not designed to describe tur-

bulence adequately inside clouds, in particular not under conditions of a small vertical wind shear. The present formulation of shallow convection has been tuned to compensate for this limitation of the turbulence parameterization. If the scheme is modified to describe turbulence better in clouds the present formulation of shallow convection will need slight adjustment (tuning) to the turbulence scheme.

The cloud cover parameterization, involving thresholds for subgrid scale condensation is also a part of the prediction problem. Cloud cover parameterization in a convective boundary layer with cumulus clouds developing into stratocumulus below a stable layer aloft is potentially problematic close to 100 % relative humidity under the stable layer. This is due to a steep slope of 'fractional cloud cover' close to saturation. The cloud cover determined with the present model in this situation is the maximum of stratiform and convective cloud cover. The details of a given cloud parameterization are clearly of some importance in the cloud prediction problem.

The complex cloud prediction problem involving all processess contributing to the heat and moisture budget of the cloud suggests that it is relevant to study the time evolution of stratocumulus using alternative physical parameterizations, in particular with regard to the treatment of turbulence, convection and cloud cover. The overall goal should be to obtain a completely coherent parameterization of the vertical subgrid scale transports from small scale turbulence to convective transports on larger vertical scales. The transports should operate in a satisfactory way in both unsaturated and moist saturated conditions.

Despite the limitations associated with the present study, the results of the experiments indicate that the new formulation of shallow convection across a stable layer is an important enhancement of the current physical parameterizations.

Acknowledgement

Thanks to Per Undén and Karl-Ivar Ivarsson for their careful reading of the original manuscript.

References

Albrecht, B., Penc, R., and Schubert, W. (1985). An observational study of cloud-topped mixed layers. *J. Atmos. Sci.*, 42:800–822.

Albrecht, B. A., Bretherton, C., Johnson, D., Scubert, W. H., and Frisch, A. S. (1995). The atlantic stratocumulus transition experiment. *Bul. Amer. Meteorol. Soc.*, 76:889–904.

Bougeault, P. (1985). The diurnal cycle of the marine stratocumuluss layer: A higher-order model study. *J. Atmos. Sci.*, 42:2826–2843.

Bretherton, C., Austin, P., and Siems, S. (1995). Cloudiness and marine boundary layer dynamics in the astex lagrangian experiments. part ii: Cloudiness, drizzle, surface fluxes, and entrainment. *J. Atmos. Sci.*, 52:2724–2735.

Bretherton, C. and Pincus, R. (1995). Cloudiness and marine boundary layer dynamics in the astex lagrangian experiments. part1: Synoptic setting and vertical structure. *J. Atmos. Sci.*, 52:2707–2723.

Charnock, H. (1955). Wind stress on a water surface. *Quart. J. Roy. Meteorol. Soc.*, 81:639–640.

Chen, C. and Cotton, W. (1983). A one-dimensional simulation of the stratocumulus-capped mixed layer. *Boundary-Layer Meteorol.*, 25:289–321.

Cuxart, J., Bougeault, P., and Redelsperger, J.-L. (2000). A turbulence scheme allowing for meso-scale and large-eddy simulations. *Quart. J. Roy. Meteorol. Soc.*, 126:1–30.

Deardorff, J. (1980). Cloud-top entrainment instability. *J. Atmos. Sci.*, 37:131–147.

Duynkerke, P. and Driedonks, A. (1988). The turbulent structure of a shear-driven stratus-topped atmospheric boundary layer. *J. Atmos. Sci.*, 45:2343–2351.

Duynkerke, P., Zhang, H., and Jonker, P. J. (1995). Microphysical and turbulent structure of nocturnal stratocumulus as observed during astex. *J. Atmos. Sci.*, 52:2763–2777.

Holtslag, A., Lenderink, G., Siebesma, P., and Sass, B. (1999). Report on turbulence evaluation meeting, knmi, de bilt. *Hirlam Newsletter*, 31:7–11.

Kuo, H.-C. and Schubert, W. H. (1988). Stability of cloud topped boundary layers. *Q.J.R. Meteorol. Soc.*, 114:887–916.

MacVean, M. (1993). A numerical investigation on the criterion for cloud-top entrainment instability. *J. Atmos. Sci.*, 50:2481–2495.

MacVean, M. and Mason, P. (1990). Cloud-top entrainment instability through small-scale mixing and its parameterization in numerical models. *J. Atmos.Sci.*, 47:1012–1030.

Moeng, C.-H., Lenschow, D., and Randall, D. (1995). Numerical investigations of the roles of radiative and evaporative feedbacks in stratocumulus entrainment and breakup. *J. Atmos. Sci.*, 52:2869–2883.

Nicholls, S. (1984). The dynamics of stratocumulus: aircraft observations and comparisons with a mixed layer model. *Q.J.R. Meteorol. Soc.*, 110:783–820.

Nicholls, S. and Leighton, J. (1986). An observational study of the structure of stratiform cloud sheets, part i: Structure. *Q.J.R. Meteorol. Soc.*, 112:431–460.

Nielsen, N. W. and Amstrup, B. (2001). DMI-HIRLAM verification report for the fourth quarter of 2000. DMI intern rapport 00-4, Danish Meteorological Institute.

Price, J. (1999). Observations of stratocumulus cloud break-up over land. *Q.J.R. Meteorol. Soc.*, 125:441–468.

Randall, D. (1980). Conditional instability of the first kind upside-down. *J. Atmos. Sci.*, 37:125–130.

Randall, D. (1984). Stratocumulus cloud deepening through entrainment. *Tellus*, 36A:446–457.

Randall, D., Shao, Q., and Moeng, C.-H. (1992). A second order bulk boundary layer model. *J. Atmos. Sci.*, 49:1903–1923.

Roach, W. and Slingo, A. (1979). A high resolution infra-red radiative transfer scheme to study the interaction of radiation with cloud. *Q.J.R. Meteorol. Soc.*, 105:603–614.

Rodgers, D. P. and Telford, J. (1986). Metastable stratus tops. *Q. J. R. Meteorol. Soc.*, 112:481–500.

Rogers, R. (1976). *A short course in cloud physics.* Pergamon Press.

Sass, B. H., Nielsen, N. W., Jørgensen, J. U., Amstrup, B., and Kmit, M. (2000). The operational DMI-HIRLAM system. Dmi tech. rep. no. 00-26, Danish Meteorological Institute.

Siems, S., Bretherton, C., Baker, M., Shy, S., and Breidenthal, R. (1990). Buoyancy reversal and cloud-top entrainment instability. *Q. J. R. Meteorol. Soc.*, 116:705–739.

Slingo, A., Brown, R., and Wrench, C. L. (1982a). A field study of nocturnal stratocumulus; III high resolution radiative and microphysical observations. *Quart. J. Roy. Meteorol. Soc.*, 108:145–165.

Slingo, A., Nicholls, S., and Schmetz, J. (1982b). Aircraft observations of marine stratoculumus during JASIN. *Quart. J. Roy. Meteorol. Soc.*, 108:833–856.

Slingo, A. and Schrecker, H. (1982). On the shortwave radiative properties of stratiform water clouds. *Quart. J. Roy. Meteorol. Soc.*, 108:407–426.

Turton, J. and Nicholls, S. (1987). A study of the diurnal variation of stratocumulus using a multiple mixed layer model. *Q.J.R Meteorol. Soc.*, 113:969–1009.

Wang, Q. and Albrecht, B. (1994). Observations of cloud-top entrainment in marine stratocumulus clouds. *J.Atmos.Sci.*, 51:1530–1547.

Wang, Q. and Lenschow, D. (1995). An observational study of the role of penetrating cumulus in a marine stratocumulus- topped boundary layer. *J. Atmos. Sci.*, 52:2778–2787.

Weaver, C. and Pearson, R. (1990). Entrainment instability and vertical motion as causes of stratocumulus breakup. *Q. J. R. Meteorol. Soc.*, 116:1359–1388.